UNIVERSITÀ DEGLI STUDI DI PADOVA

Scuola di Dottorato di Ricerca in Fisica
XXX Ciclo

RESILIENCE, COMPLEXITY AND COOPERATION IN SOCIO-ECOLOGICAL SYSTEMS

-

Direttore della Scuola: PROF. GIANGUIDO DALL'AGATA

Supervisore: DR. SAMIR SUWEIS

Co-supervisore: PROF. AMOS MARITAN

Candidato: CHENGYI TU

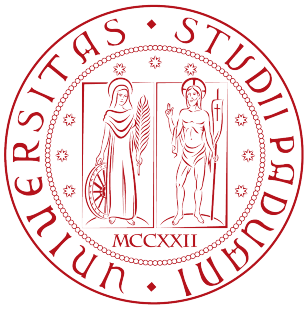

Dipartimento di Fisica e Astronomia 'G. Galilei'

CONTENTS

0 INTRODUCTION

In order to properly understand the big picture, everyone should fear becoming mentally clouded and obsessed with one small section of truth.

— Xun Kuang (310 BC - 237 BC)

0.1 RESILIENCE, COMPLEXITY AND COOPERATION IN SOCIO-ECOLOGICAL SYSTEMS

Advances in experimental technologies, both in the laboratory and in the field, are generating an increasing volume of ecologically and sociologically relevant data [1, 2, 3, 4, 5, 6], spanning a wide range of scales, revealing recurrent emergence of patterns [7, 8, 9, 10] in these systems. This "data explosion" is both a challenge (inventing new tools for their analysis [11, 12, 13, 14]) and an opportunity (identifying rules driving the functioning of complex systems [15, 16, 17, 18]). However, data alone do not necessarily lead to an understanding of the systems of interest. At present, we are in a situation where in front of a rich (but common to many systems) phenomenology we have innumerable models for very specific cases that call for a general vision [19, 20]. This challenge is very fascinating for physicists, that have in their veins the search for general principles of apparently different phenomena.

In particular, a very important property that seems to be shared by most of the socio-ecological systems is their ability to respond to perturbations, i.e. the system resilience. Cell biology [21, 22], ecology [23, 24, 25], environmental science [26, 27], and food security [28, 2] are just some of the many areas of investigation [29, 4, 3] on the mechanisms increasing the system resilience. Nevertheless, not all socio-ecological systems display high resilience. In food security, the intensification of international food trade and local shocks in food production led to global food crises, and for example Ref. [2] develops a framework to investigate the coupled global food-population dynamics and finds that the global food system is losing resilience (increasingly unstable and susceptible to conditions of crisis); In ecology, the concept of resilience has evolved considerably since Holling's (1973) seminal paper [30] to describe the persistence of natural systems in the face of changes in ecosystem variables due to natural or anthropogenic causes. It has been suggested that in many ecosystems we are facing a lost of resilience and consequent loss of biodiversity [31, 32, 33]. Therefore an important challenge is to understand what

are the main drivers ruling the resilience of ecological communities, so that proper ecosystem management strategy can be developed [34].

From data is emerging that one of the key feature of socio-ecological system resilience may lie in the architecture of the interaction networks. The topology of the interaction network may actually represent the "parameter" that system somehow self-tunes so that the system's responses to stimuli is optimized with respect to some feature (e.g. stability). In inanimate matter, spins or particles always have their mutual interactions turned on (with an intensity decaying with their relative distance) and the network describing their interaction is dense, with most of the connections present. In contrast, if we consider for instance an ecosystem, species interact selectively even if they coexist at short distances, and the species interaction network is sparse, that is, most of the interactions are turned off. At the same time, the interactions that are turned on form non-random evolving structures that are the result of some optimization process under adaptive/evolution pressure [35, 7]. Thanks to massive databases now easy available, characteristics similar to those just mentioned for ecological networks, have been observed also in gene-interaction network [36, 37, 38], in neuronal networks [39, 40, 41] and even in social networks [42, 4, 43]. These networks are very different and yet share a crucial aspect: they all have undergone biological/social evolution that has driven their incremental complexity.

One particular long-standing question regards the relationship between stability (resilience) and complexity in ecological system. Many of the population dynamics modeling frameworks proposed in the literature [44, 45, 46] cannot elude the celebrated May's theorem [47]. This theorem, recently refined by Allesina and Tang [23] states that the stability of the system depends on the product SC, where S is the number of species and C is the fraction of non-zero pairwise interactions between species. This result leads to the so-called stability and complexity paradox debate [45]: a system in order to be stable cannot be too large (S large) or too connected (large C). The paradox lies in the fact that empirically, ecosystems with a large number of species seem to be very stable [48, 45]. Moreover, recently it has been suggested that because of this stability paradox, in microbial ecosystems competition may play a much important roles than what expected until now. In fact in these models, competition has a stabilizing role in ecosystem dynamics, contrarily to cooperation that decreases the ecosystem resilience [49, 50].

During my Ph.D. I have used a physicists approach based on complex networks and statistical physics, to study the resilience in Socio-Ecological systems, how it is related to the system complexity and what is the role of cooperation in the ecosystem dynamics. I have used a comprehensive approach that includes data mining, theoretical modeling (both computational and analytical) and statistical anal-

yses. In particular, I have investigated the efficiency of a recently proposed framework to study the resilience of complex interacting systems, what the role of cooperation and competition in the universal patterns theoretically predicted by the model, and its validation with data. I have then focused on the long-standing open question of the relation between complexity and resilience in ecosystems, by specifically focusing on how the architecture of interaction networks may confer to living systems their ability to promptly react to to perturbations (e.g. increase resilience). To do that we have developed a stochastic population dynamics model, generalizing an interacting non-equilibrium model known as the voter model [51, 52, 53], and I have also studied the effect of cooperation on the ecosystem resilience. The results of my work suggest a novel picture on the relation between complexity, cooperation and resilience, challenging previous results in the literature [23, 7, 49, 50].

0.2 THESIS OUTLINE

The thesis blends and integrates the material published in a series of peer-reviewed or preprinted publications, and it is organized in seven brief chapters. A general introduction outlines the conceptual thread joining the various issues studied. The other chapters are tailored from the published works as outlined in detail below. A set of conclusions, putting forth perspectives and further possible developments, and the Appendices - where I have explained some mathematical technicalities - are integral part of this thesis work. In the first part, Chapters 1 2 3, we introduce a general theoretical framework that allows to predict and explore the resilience of network-based complex systems and discuss the properties of the interactions to determine the accuracy of the approximation. This part is rewritten from Tu C, Grilli J, Schuessler F, et al. "Collapse of resilience patterns in generalized Lotka-Volterra dynamics and beyond", Physical Review E, 2017, 95(6): 062307; The second part, Chapters 4 5 6, we propose an ecological stochastic model which is appropriate for species communities with mutualistic/commensalistic interactions and find that, in the large system size limit, any number of species can coexist for a very general class of interaction networks and that the stationary state is globally stable. This part is rewritten from Tu C, Suweis S, Grilli J, et al. Cooperation promotes biodiversity and stability in a model ecosystem. arXiv preprint arXiv:1708.03154, 2017., in review.

Part I

NETWORK RESILIENCE AND ITS ACCURACY

Simulated disorder postulates perfect discipline; simulated fear postulates courage; simulated weakness postulates strength.

— Lao Tzu (? - 531 BC)

1 RESILIENCE OF COMPLEX SYSTEMS DYNAMICS

All difficult things have their origin in that which is easy, and great things in that which is small.

— Lao Tzu (? - 531 BC)

1.1 THE CONCEPT OF RESILIENCE

The fundamental agents of biological or socio-economic systems, from genes in gene-regulatory networks to stock holders in financial markets, act under complex interactions and in general we do not know how to derive the dynamic from first-principle potentials. In general these interactions are described by pair-wise relations through a matrix (the adjacency matrix) that regulates, typically in non-linear way, the effect of the interactions to the dynamic of the single component.

In particular, there is a rising interest in assessing how interactions determine the stability (or resilience) of dynamical attractors [54], i.e. the ability of a system to return after a perturbation to the original equilibrium state [1, 55, 5, 23]). Cell biology [21, 22], ecology [23, 24, 25], environmental science [26, 27], and food security [28, 2] are just some of the many areas of investigation [29, 4, 3] where the relation between interaction properties and stability is, although deeply studied, a central open question. Therefore, understanding the role of system topology in resilience theory for multi-dimensional systems is an important challenge from which our ability to prevent the collapse of ecological and economic systems, as well as to design resilient system.

1.2 CLASSIC ONE-DIMENSIONAL METHOD TO QUANTIFY RESILIENCE IN ONE DIMENSIONAL SYSTEMS

We start by presenting the traditional mathematical method to quantify resilience in one-dimensional systems driven by the non-linear dynamic equation

$$\frac{dx}{dt} = f(\beta, x) \tag{1}$$

where $f(\beta, x)$ represents the system's dynamic and β is the (control) parameter to capture the variable conditions. If for a stable fixed points of Eq. (1), x^*, the following conditions hold:

$$f(\beta, x^*) = 0, \tag{2}$$

$$\lambda = \frac{\partial f}{\partial x}|_{x=x^*} < 0, \tag{3}$$

then the solution of these conditions is called resilience function

$$x(\beta). \tag{4}$$

Eq. (2) and (3) guarantee that the system is in its steady state and that is linearly stable around it, i.e. for small perturbations the system will go back to the un-perturbed equilibrium point x^*. In this case, Eq. (4) represents the possible states of the system as a function of the control parameter β.

The shape of the resilience function (see Fig. 1) is given by Eq. (4) and uniquely determined by the functional form of $f(\beta, x)$. If it is folded backwards, then three equilibria may exist depending on the value of the control parameter β. The colored lines in the $\beta - x$ plane represent the equilibrium solutions, i.e. the values $x^*(\beta)$ such that $f(\beta, x^*) = 0$. The black arrows in each sub-figure indicate the direction in which the system moves if it is not in the equilibrium. It can be seen from these arrows that all curves represent stable equilibria, except for the yellow middle section. In this case, if the system is driven slightly away from this part of the curve, it will move further away instead of returning. At the critical point β_c of Eq. (4) the system Eq. (1) loses its resilience by undergoing a sudden transition to a different and often undesirable fixed point. This is known as critical transition and it is a well studied phenomena in complex system literature [6, 56, 57, 58, 13].

Therefore, in one dimensional dynamic, as far as the function f is invertible, a complete analytical treatment of the resilience of the system is possible. We can identify the critical value of the control parameter β and study the effect of external perturbation to the system. Typically one is interested to study how to anticipate or avoid critical transitions in the system and to this respect many indicators have been developed.

1.3 CRITICAL SLOWING DOWN

One of the most used indicator in known is critical slowing down (CSD). In dynamical system, the phenomenon of CSD is indeed a good indicator of whether the system approach to a critical threshold [59]. For example in Fig. 1, if the system approaches the fold bifurcation point β_c, the dominant eigenvalue characterizing the rates of change around the equilibrium becomes zero, and consequently the recovery rates decrease smoothly to zero [60, 13, 12] (Fig. 2). CSD tends to lead to an increase in the AR1 (lag-1 autocorrelation) [15] and variance [16] of the fluctuations in a stochastically forced system

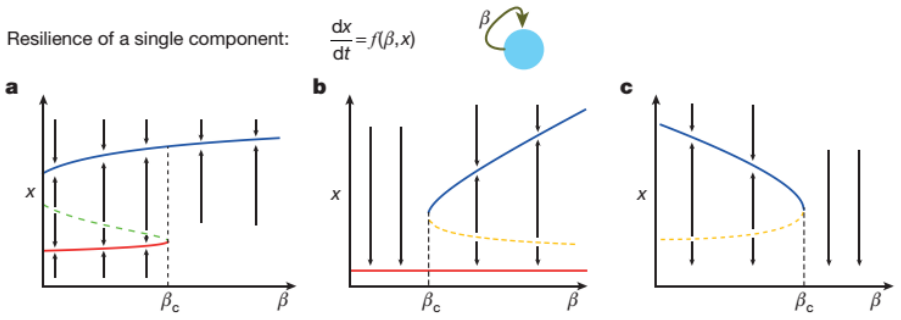

Figure 1: Three typical examples of resilience function for one-dimensional system where the blue/red branch represents the desired/undesired stable fixed point. The yellow branch represents the unstable fixed point. The arrows represent the direction driving the system to the stable fixed point. a, Resilience function displaying a bifurcation. If $\beta > \beta_c$, there is only a single stable state (blue curve); If not, there is one desired stable state (blue curve) and another undesired state (red curve). b, Resilience function displaying a first order transition from the desired state (large x^*) to the undesired state $x^* \to 0$. c, Resilience function displaying a stable state for $\beta < \beta_c$ and no solution above β_c. [extract from [11]]

approaching a bifurcation for the critical value of the control parameter.

For simplicity, let us consider the 1-dimensional system given by Eq. (1) but for discrete time steps, and let us call $\bar{x}$ its equilibrium at stationarity. If we assume to perturb the system around $\bar{x}$ and we quantify the deviation of the state variable x from the equilibrium the time step n as $y_n = x_n - \bar{x}$, then we can describe the dynamic of y_n through the linearizion of the dynamic around $\bar{x}$, i.e. $y_{n+1} = y_n + \lambda y_n$. Then, after a period Δt we have that $y_{n+1} = e^{\lambda \Delta t} y_n$, i,e. the return to equilibrium is approximately exponential with a certain recovery speed λ. If we add to the solution a Gaussian noise mimicking continuous perturbation to the stationary solution, then the previous equation becomes $y_{n+1} = e^{\lambda \Delta t} y_n + \sigma \epsilon_n$ where ϵ_n is a random number from a standard normal distribution and σ is the standard deviation. If λ and Δt are independent of y_n, this model is a first-order autoregressive process $y_{n+1} = \alpha y_n + \sigma \epsilon_n$ where $\alpha = e^{\lambda \Delta t}$ is the autocorrelation. The expectation and standard deviation of the classic first-order autoregressive process $y_{n+1} = c + \alpha y_n + \sigma \epsilon_n$ is $E(y_{n+1}) = E(c) + \alpha E(y_n) + E(\sigma \epsilon_n) \Rightarrow \mu = c + \alpha \mu + 0 \Rightarrow \mu = \frac{c}{1-\alpha}$ and $Var(y_{n+1}) = E(y_{n+1}^2) - \mu^2 = \frac{\sigma^2}{1-\alpha^2}$. When the system approaches to the critical point, the return speed to equilibrium decreases (λ approaches zero), the autocorrelation α tends to one and the variance tends to infinity.

Briefly, in the dynamic of a system approaching a bifurcation, CSD leads to (1) slower recovery from perturbations, (2) increased autocor-

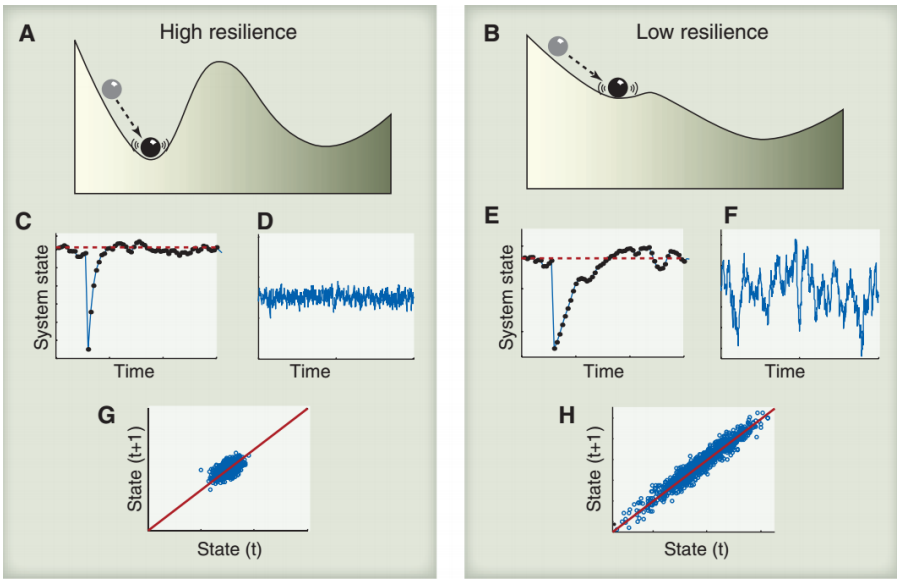

Figure 2: CSD is an indicator that the system has lost resilience. When the system is far from/close to the bifurcation point (A/B), its resilience is high/low, i.e. the basin of attraction is large/small (C/E), the rate of recovery from perturbations is relatively high-/low (D/F) and the resulting dynamic are characterized by high-/low correlation between the states at subsequent time intervals (G/H). [extract from [13]]

relation and (3) increased variance. All these indicators can be used to detect early warning of critical transitions [12].

2 NETWORK RESILIENCE

He who controls others may be powerful, but he who has mastered himself is mightier still.

— Lao Tzu (? - 531 BC)

2.1 HOW TO ESTIMATE THE RESILIENCE OF COMPLEX NETWORK?

The classic one-dimensional method [54] presented above assumes that the system dynamics can be approximated by one-dimensional equation (1) $\frac{dx}{dt} = f(x, \beta)$, where β represents the endogenous effects on the system. Although this method is conceptually powerful, it has very limited applicability on "real world" problems, as it is unable to account for resilience of complex multi-dimensional system composed of numerous components interacting via a complex network of weighted edges.

The CSD method could in theory inform about the critical point also of multidimensional complex system, but being an approximated numerical method, it is also presents many limitations, as difficult to control sensitivity on the system parameters, high computational costs (exponentially increasing) for investigating the critical transition for several different combination of the system parameter. Additionally, it does not offer the testable predictions for the system's response to different perturbations, not giving insights that allow to design optimal resilient multidimensional systems.

Recently, Gao et al. [11] overcome these drawbacks by developing a general theoretical framework that allows us to predict and explore the resilience of network-based complex system and open a new way to understand the resilience in complex natural and man-made systems.

They consider a class of equations describing the dynamics of several types of multi-dimensional systems (ranging from cellular [61] to ecological [62, 7] and social systems [63]) with pair-wise interactions:

$$\dot{x}_i = F(x_i) + \sum_{j=1}^{S} A_{ij} G(x_i, x_j) \tag{5}$$

where $\mathbf{x} = (x_1, ..., x_S)$ is the activities of S components/nodes, the functions $F(x_i)$ and $G(x_i, x_j)$ represent the intrinsic dynamics of node i and its dynamics driven by the interaction with the other components, respectively. Finally, the weight matrix A_{ij} specifies the interaction between nodes: if $A_{ij} = 0$, then there is no interaction between

i and j; otherwise the edge weight A_{ij} represents the strength of the interaction from j to i.

In analogy with the 1D system of equation [64, 65, 4], a transition from a desired to an undesired stable fixed point captures the loss of resilience also in the multi-dimensional system of equation (4). The key difference is that equation (5) is not controlled only by one parameter (e.g. β), but it depends on many parameters, such as the weights of all edges, the parameters of self-dynamics $F(x_i)$ and those characterizing the inter-dynamics $G(x_i, x_j)$. Therefore, the resilience loss can be induced by changes in any of the S^2 parameters, with each change capturing a different kind of perturbation (see Fig. 3). For instance, the extinction of species in an ecological system may correspond to the removal of one or several nodes [11]. Therefore, the resilience function of complex network is a multi-dimensional manifold over the parameter space characterizing the system.

2.2 FRAMEWORK OF ONE-DIMENSIONAL EFFECTIVE EQUATION

Characterizing the analysis in Gao et al. [11], the average nearest neighbour activity x_{eff} and effective control parameter β_{eff} of Eq. (5) are given by (see Appendix A for details):

$$x_{eff} = \frac{\mathbf{1}^T \mathbf{A} \mathbf{x}}{\mathbf{1}^T \mathbf{A} \mathbf{1}} = \frac{\sum_{ij} A_{ij} x_j}{\sum_{ij} A_{ij}} \tag{6}$$

$$\beta_{eff} = \frac{\mathbf{1}^T \mathbf{A} \mathbf{s}^{in}}{\mathbf{1}^T \mathbf{A} \mathbf{1}} = \frac{\sum_{ij} A_{ij} A_{ji}}{\sum_{ij} A_{ij}}. \tag{7}$$

We highlight that β_{eff} is the average over the product of the out-degrees and in-degrees of all nodes, and thus now depends on the whole network topology. The dynamics of x_{eff} following Eq. (5) can be mapped through Eq. (79) to a one-dimensional effective equation:

$$\dot{x}_{eff} = f(\beta_{eff}, x_{eff}) = F(x_{eff}) + \beta_{eff} G(x_{eff}, x_{eff}), \tag{8}$$

where β_{eff} is the control parameter. By solving the equilibrium state of this equation ($f(x_{eff}, \beta_{eff}) = 0$), one could obtain the resilience curve $x(\beta)$ or $\beta(x)$ in the two dimensional coordinate system. For the one-dimensional system given by Eq. (8), the resilience function $x(\beta)$ is calculated analytically and uniquely determined by $f(x, \beta)$, which represents the possible states of the system as a function of the parameter β_{eff}.

Summarizing, in order to study the resilience or the existence of critical transitions of the complex multi-dimensional system given by Eq. (5), one could simply calculate β_{eff} from the network and analyze the corresponding resilience function $x(\beta_{eff})$ of Eq. (8). Clearly, the properties of the one-dimensional non-linear Eq. (8) could be studied

easily and the original S^2 parameters of the microscopic description A have been collapsed into a single macroscopic resilience parameter β_{eff}, so this framework is conceptually powerful. Of course it also presents some important limitations that will be described later in the next Chapter.

2.3 RESILIENCE OF ECOLOGICAL DYNAMICS

In this section we will apply the above theoretical framework to a potential "real world" case of interest, namely the dynamics of ecological species interacting through mutualistic relationships. Mutualistic networks have been intensively studied in recent years [24, 7, 66, 67, 68, 69, 70]. In particular, it has been shown [67] that these type of ecological communities display characteristic network architecture, named "nested", i.e. a topological structure in which specialist species tend to be connected with generalists one, forming a hierarchy from the generalist to the specialist. It has suggested that this type of structures minimizes competition [69], confers robustness against species loss and other systemic damages [68]. Nevertheless, other studies have demonstrated that structured mutualistic ecological networks are less stable than their random counterparts [7] and that nestedness is detrimental to community stability [23, 24]. Therefore, the relationship between mutualistic networks and resilience is still an open problem. Here we want to review some results on critical transitions in these systems as a function of the network perturbation intensity.

2.3.1 *The model*

Following the work of Gao and collaborators [11], we describe the population dynamics of the mutualistic community as follow:

$$\frac{dx_i}{dt} = B_i + x_i\left(1-\frac{x_i}{K_i}\right)\left(\frac{x_i}{C_i}-1\right) + \sum_{j=1}^{S} A_{ij}\frac{x_i x_j}{D_i + E_i x_i + H_j x_j} \quad (9)$$

where x_i is the abundance of species i, the first term B_i represents the constant incoming migration, the second term $x_i\left(1-\frac{x_i}{K_i}\right)\left(\frac{x_i}{C_i}-1\right)$ represents logistic growth with the carrying capacity K_i [71] and Allee effect C_i [72] and the third term represents the mutualistic contribution from species x_j to x_i. We highlight that the above Eq. (9) is a specific example of the general class of equations given by Eq. (5) with $F(x_i) = B_i + x_i\left(1-\frac{x_i}{K_i}\right)\left(\frac{x_i}{C_i}-1\right)$ and $G(x_i, x_j) = \sum_{j=1}^{S} A_{ij}\frac{x_i x_j}{D_i + E_i x_i + H_j x_j}$ only if all the parameters do not depend on the specific species. In the following we will work within this assumption and with fixed parameters values, i.e. $B = B_i = 0.1$, the Allee effect $C = C_i = 1$, carrying capacity $K = K_i = 5$ and $D = D_i = 5$, $E = E_i = 0.9$, $H = H_j = 0.1$.

2.3.2 *Empirical networks*

Some empirical ecological networks describing the mutualistic interaction, especially plant-pollinator relationships among species, have been collected by ecologists [73, 74, 75, 76] and available on the web [77]. Each empirical species interaction network is described by a matrix M representing a $n \times m$ bipartite graph comprising n plants/-fishes and m pollinators/anemones. From M_{ik} we construct two projection networks A_{ij} and B_{ij} can be constructed by linking pairs of plants that share mutual pollinators (A_{ij}), or pollinators that share mutual plants (B_{ij}). If the pollinator k pollinates two plants i and j, then we assign a weight to the link between these two plants of strength $\frac{M_{ik}M_{jk}}{\sum_{s=1}^{n} M_{sk}}$. Further, if there are many mutual pollinators k that plants i and j share, then the mutualistic interaction between them will be stronger. Therefore, the weighted plant network can be constructed by: $A_{ij} = \sum_{k=1}^{m} \frac{M_{ik}M_{jk}}{\sum_{s=1}^{n} M_{sk}}$. A similar procedure is used to construct the weighted pollinator network B_{ij}.

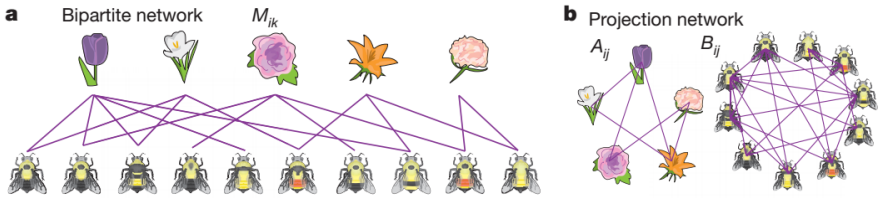

Figure 3: a, The bipartite network M consists of nodes representing mutualistic interactions, such as plant/fish and pollinator/anemone. b, The two projected network (A - plants that share mutual pollinators and B - pollinators that share mutual plants) from the bipartite graph M. [extract from [11]]

2.3.3 *Numerical simulations*

For testing the resilience under realistic perturbations, each network is perturbed through the following three methods:

1. Node perturbation. First, remove a fraction f_n of nodes in the network A randomly; Second, capture the giant connected component; Third, re-run the numerical simulation again. This perturbation simulates the extinction of plant/pollinator;

2. Link perturbation. First, remove a fraction f_l of links in the network M randomly; Second, re-construct the plant and pollinator network A and B; Third, re-run the numerical simulation again. This perturbation simulates the disappearance of mutualistic link;

3. Global perturbation. First, generate random variate r_{ij} from a uniform distribution with mean $f_w < 1$; Second, shift the link weight A_{ij} by the factor r_{ij}; Third, re-run the numerical simulation again. This perturbation simulates a global change in the environmental conditions, for example, varying temperature.

For testing whether the fixed points are stable, each network includes three different initial state:

1. low initial state x_L, where all $x_i(t = 0) = 10^{-3}$;
2. high initial state x_H, where all $x_i(t = 0) = 6$;
3. random initial state x_R, where $x_i(t = 0)$ is a random variate from the uniform distribution between 0 and 10.

Each network and initial condition are substituted to Eq. (9) and we solve numerically the system of coupled differential equation after each perturbation. The results are summarized in Fig. 4. For different perturbations (node perturbation, link perturbation and global perturbation, respectively) of the same system, the corresponding resilience pattern is different. For different ecological system to which we apply the same perturbation procedure, the corresponding resilience patterns are also different. When the perturbation is small, the system maintains its resilience. If the perturbation exceeds a certain threshold, the occurrence of bifurcation leads to a critical transition, from the desired state x_H and an undesired one x_L. However, owing to the multi-dimensionality of A_{ij}, each realization is microscopically distinct, and as a result the bifurcation point is unpredictable across different realizations. Therefore, system loses its resilience under some highly unpredictable conditions.

2.3.4 *Universal resilience patterns in complex networks*

The network resilience depends on the network topology, perturbation and specific realization. This seemingly unpredictable and elusory behaviour can be systematically treated by the one-dimensional effective mean field equation presented above. Reducing the multi-dimensional Eq. (9) to the form of Eq. (8), one obtains the following one-dimensional effective equation:

$$f(\beta_{eff}, x_{eff}) = B + x_{eff}\left(1 - \frac{x_{eff}}{K}\right)\left(\frac{x_{eff}}{C} - 1\right) + \beta_{eff}\frac{x_{eff}^2}{D + (E + H)x_{eff}} \tag{10}$$

Its fixed points can be found by $f(\beta_{eff}, x_{eff}) = 0$, namely

$$\beta_{eff}(x_{eff}) = -\left[B + x_{eff}\left(1 - \frac{x_{eff}}{K}\right)\left(\frac{x_{eff}}{C} - 1\right)\right]\frac{D + (E + H)x_{eff}}{x_{eff}^2}$$

(11)

which describes β_{eff} by function of x_{eff}. Inverting the above equation, one could obtain the final curve in the $\beta_{eff} - x_{eff}$ two-dimensional space, which describes the stationary solution for x_{eff} as a function of β_{eff}. The system linear stability is thus guaranteed when $\frac{\partial f(\beta_{eff}, x_{eff})}{\partial x_{eff}} < 0$.

As shown in Fig. 5, the resilience shows two different regimes, separated by a critical transition at β^c_{eff}:

1. $\beta_{eff} > \beta^c_{eff}$. The system has a single fixed point x_H;
2. $\beta_{eff} < \beta^c_{eff}$. The system features three potential fixed points, x_H, x_L and the intermediate x_M.
   a) In the top regime, the system is resilient as long as x_H could recover from the disturbance deviating it.
   b) In the middle regime, the system is unstable due to positive slope, $\frac{\partial f(\beta_{eff}, x_{eff})}{\partial x_{eff}} > 0$. Therefore any perturbation driving the system below x_M will lead to resilience loss.
   c) In the bottom regime, if the perturbation is large enough, the system may lose resilience, potentially transitioning between the three states x_H, x_M and x_L.

At the critical value, β^c_{eff}, the two lower fixed points, x_L and x_M are merged into a single point x^c_{eff}. For obtaining the critical point β^c_{eff}, β^c_{eff} and x^c_{eff} must satisfy the following two conditions:

$$\begin{cases} \frac{\partial f(\beta^c_{eff}, x_{eff})}{\partial x_{eff}}|_{x^c_{eff}} = 0 \\ f(\beta^c_{eff}, x^c_{eff}) = 0 \end{cases} \tag{12}$$

The critical point of this bifurcation in our case is $(\beta^c_{eff}, x^c_{eff}) = (6.97, 0.20)$, a value fully determined by the dynamics, independent of the network topology.

By mapping the results of all realizations of Fig. 4 into the Fig. 5, all points collapse into a single universal curve in the two-dimensional state space $\beta_{eff} - x_{eff}$, no matter the specific network topology, perturbation and realizations have been chosen. This result shows the universality of the resilience patterns in the one dimensional reduced space, indicating that the mean field approximation works well in this case.

2.4 CONCLUSION

In summary, the resilience patterns of the multi-dimensional system dynamics given by Eq. (5) are diverse and unpredictable because of the inherently high-dimensional of the parameter space. By mapping

the system into a two-dimensional $\beta_{eff} - \varkappa_{eff}$ coordinate space, the hidden resilience universal pattern is unveiled, independently on the specific network, type of perturbation and realization. This framework, at least for a given class of multi-dimensional system dynamics equations and type of interactions, accurately predicts the system's response to diverse perturbations, correctly identifies the critical points where the system loses its resilience. It further offers potential strategies to avoid the loss of resilience and design principles for optimal resilient systems that can successfully cope with perturbations. In the next chapter we will further investigate the limits and conditions for this theoretical framework to hold.

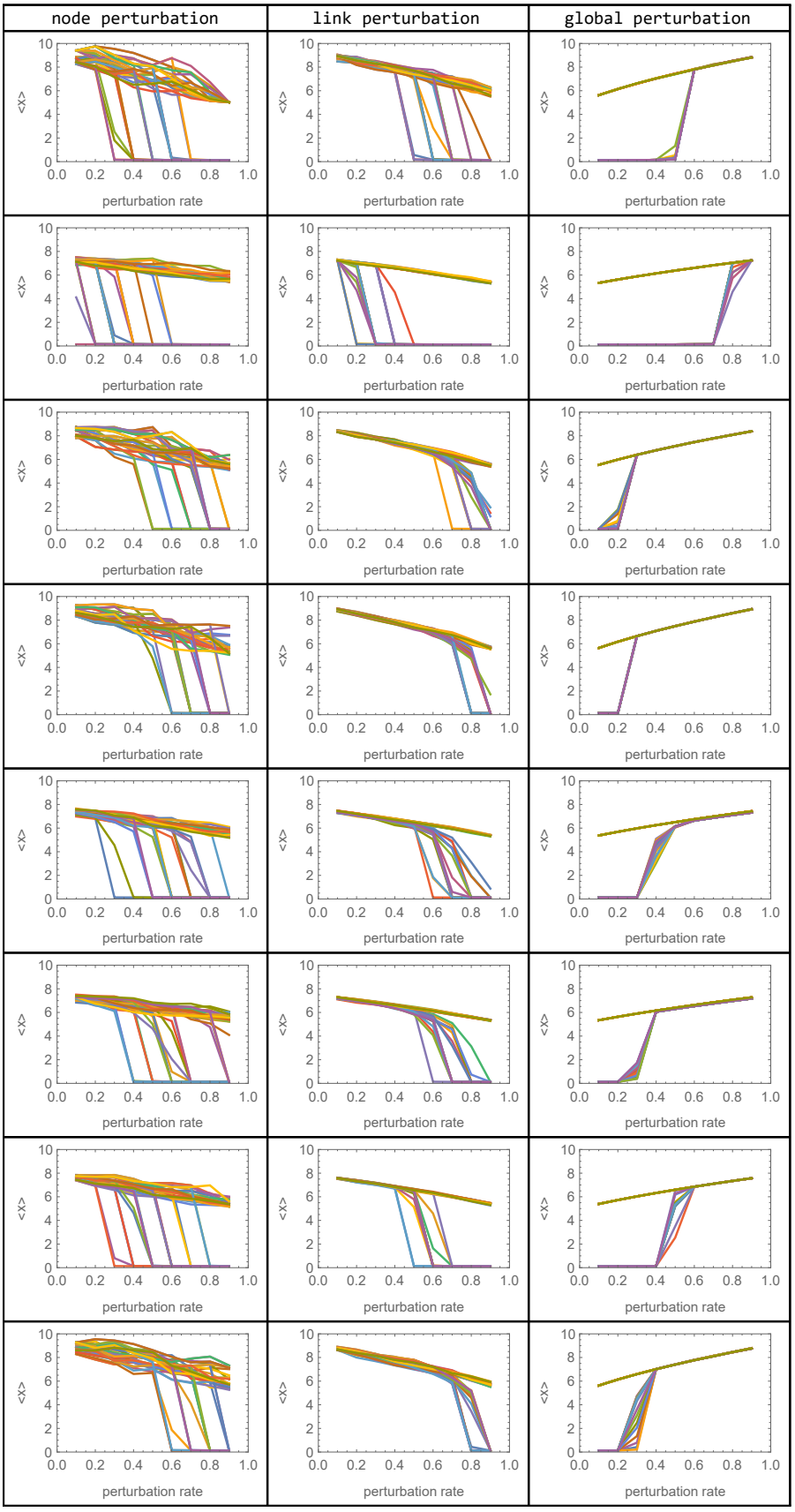

Figure 4: Resilience of mutualistic networks. Each sub-figure shows the perturbation rate vs. average abundance $\langle x \rangle$ of species in a mutualistic network following a perturbation across 100 realizations.

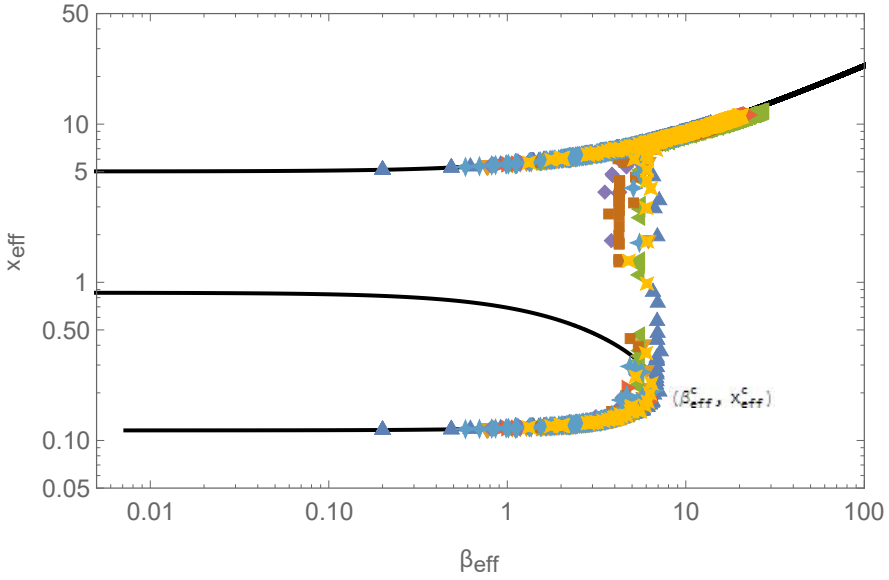

Figure 5: Collapse of all different realizations of the perturbed dynamics shown in Fig. 4 onto the universal resilience function in the $\beta_{eff} - x_{eff}$ two-dimensional space. Different colors of the points represent the different realizations of node perturbations (circles), link perturbations (squares) and global perturbations (diamonds). The black curve is the universal resilience function given by the mean field approximation and the bifurcation is predicted at $\beta^c_{eff} = 6.97$, independent of A_{ij}.

3

RESILIENCE OF GENERALIZED LOTKA-VOLTERRA DYNAMICS AND BEYOND

Those who have knowledge, don't predict. Those who predict, don't have knowledge.

— Lao Tzu (? - 531 BC)

3.1 MOTIVATION

In the previous chapter, we have presented the main results of the seminal work of Gao and collaborators [11], showing the potential hidden universality of resilience patterns for multi-dimensional systems driven by differential equations with pair-wise interactions. As detailed in Appendix A, the main conditions claimed by Gao and collaborators to be at the heart of this framework are:

(i) The network determined by the interaction between pairs of nodes has negligible degree correlations;

(ii) The node activities are uniform across nodes on both the drift and pair-wise interaction functions;

(iii) The weights of the interaction network are all positive.

Moreover, they assume that their results hold for any particular equations within the class of differential equations described by Eq. (5).

In this chapter, we consider whether these conditions are sufficient and/or necessary to guarantee that the framework works, and whether the results are independent of the model chosen. Specially, we provide - using a random matrix approach - quantitative predictions of the quality of the one-dimensional collapse as a function of the properties of interaction network and considering only stable dynamics.

The main result of this chapter are:

- We find a new condition on the network interactions that poses effective limitation to the framework.
- We show that the multi-dimensional reduction also works for interaction matrix with a mixture of positive and negative signs
- We find that only a subset of dynamics of the class given by Eq. (5) are actually valid in order to have an accurate mean-field approximation.

We prove analytically our results for generalized Lotka-Volterra and test them by numerical simulations also for more general dynamics.

3.2 GENERALIZED LOTKA-VOLTERRA DYNAMICS

The generalized Lotka-Volterra (GLV) dynamics are a set of first-order, nonlinear, differential equations frequently used to describe ecologic systems in which many species interact. Species interaction network can be used to model competition, predator-prey and mutualistic relationships between an arbitrary number of species and the species population dynamics for species i is given by

$$\dot{x}_i = \alpha_i x_i + x_i \sum_{j=1}^{S} A_{ij} x_j, \tag{13}$$

where S is the number of species in the community, x_i is the populations of species i, α_i is the intrinsic growth rate of the species i and A_{ij} is the relationships between species i and j.

The interactions in the ecological network may have positive impact (+), negative impact (-) or neutral impact (0) on the population of the tracked species. The possible combinations outcomes for pair-wise interactions allow the classification of various interaction types, as described by Fig. 6.

1. Mutualism (++). For example, two species exchange metabolic products to the benefit of both.
2. Parasitism/Predation (+-). For example, wolfs prey rabbits.
3. Amensalism (-0). For example, metabolic by-products of a microbial species alter the environment to the detriment of other microorganisms.
4. Commensalism (+0). For example, commensals cross-feed on compounds that are produced by other community members.
5. Competition (–). For example, two bacteria competing for the same resource.

The effective interactions (type and strength) between species are emergent quantities that arise from the multiple interactions among the species. If α_i is positive, then species i is able to reproduce in the absence of any other species (for example, a plant); If α_i is negative, then its population will decline unless the appropriate other species are present (for example, a herbivore that cannot survive without plants to eat, or a predator that cannot persist without its prey). If both A_{ij} and A_{ji} are negative, then the two species are in competition, since they each have a direct negative effect on the other's population.

If A_{ij} is positive but A_{ji} is negative, then species i is a predator and species j is prey, since the population of i grows at the expense of j. If both A_{ij} and A_{ji} are positive, then the two species are mutualism, since there is a relationship in which each species benefits from the activity of another one. The vectorized form of Eq. (13) is obviously $\dot{\mathbf{x}} = \mathbf{x} \circ (\boldsymbol{\alpha} + \mathbf{A} \cdot \mathbf{x})$.

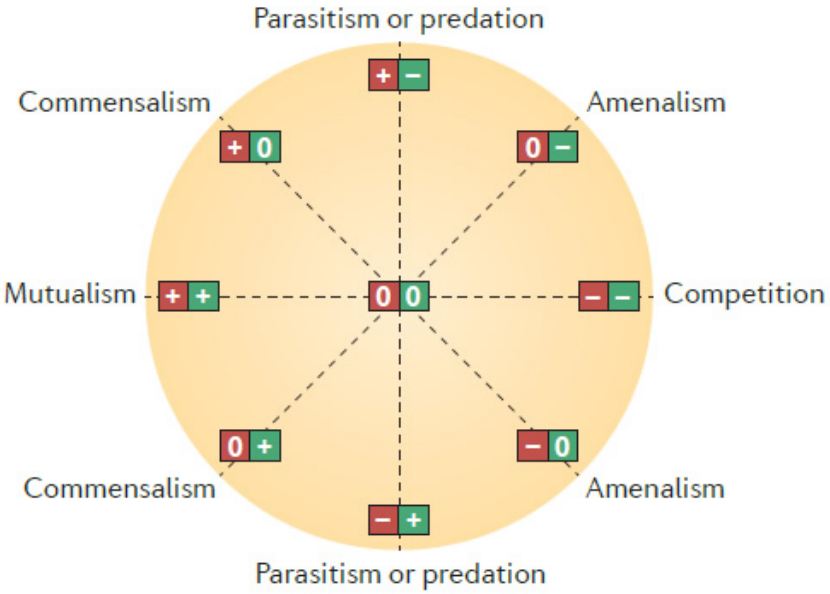

Figure 6: [Extract from [78]] Summary of ecological pair-wise interactions types between two species. For each interaction partner, there are three possible outcomes: positive (+), negative (-) and neutral (0) impact.

The Generalized Lotka-Volterra dynamics may include limit cycles, chaos and attractors and can be analyzed analytically to some extent. Its fixed points can be found by setting $\dot{x}_i = 0$ for all i, which gives $\mathbf{x}^* = -\mathbf{A}^{-1} \cdot \boldsymbol{\alpha}$ or $\mathbf{x} = 0$.

In order to better understand the conditions of the collapse presented by the above chapter, a simplified GLV dynamics where both conditions (i) and (ii) are satisfied is adopted. By considering $F(x) = \alpha x$ and $G(x, y) = xy$, the condition (ii) is valid by definition. In this case, the generalized Lotka-Volterra dynamics is defined by:

$$\dot{x}_i = \alpha x_i + x_i \sum_{j=1}^{S} A_{ij} x_j, \tag{14}$$

where α is the same for all species. On the other hand, condition (i) is always satisfied if $\mathbf{A}$ is a random matrix (see section 3.4).

The analytical solution for the stationary state of the above GLV dynamics is $\mathbf{x}^* = -\mathbf{A}^{-1} \cdot \boldsymbol{\alpha}$. Therefore, $x_{eff} = \frac{\sum_{ij} A_{ij} x_j}{\sum_{ij} A_{ij}}$ and $\beta_{eff} = \frac{\sum_{ijk} A_{ik} A_{kj}}{\sum_{ij} A_{ij}}$ could be calculated analytically as a function of properties of the weighted adjacency matrix $\mathbf{A}$ (see Eqs. (18) and (19) in

section 3.4). Moreover, this solution is globally stable if the positive orthant if **A** is positive definite [79, 25]. Finally, the corresponding one-dimensional analytical effective equation for GLV dynamics reads as $\frac{dx}{dt} = \alpha x + \beta x^2$, whose feasible ($x(\beta) > 0$) and stationary solution is:

$$x(\beta) = -\alpha/\beta, \tag{15}$$

with $\alpha/\beta < 0$. For values of $\alpha/\beta > 0$, the solution exists, but is not meaningful.

3.3 ERROR AS DISTANCE FROM THE MEAN POINT (x_{eff}, β_{eff})

In order to measure the vertical distance from the point (x_{eff}, β_{eff}) obtained from Eq. (5) and the stationary solution of the one-dimensional resilience function $x(\beta)$ (see section 3.4), we define the following function allowing us to estimate the error of the proposed approximation (see Figure 7):

$$err_x = \left| \frac{x_{eff} - x(\beta_{eff})}{x_{eff}} \right| \tag{16}$$

Similarly, to measure the horizontal distance from this point to the same resilience curve, we also define the horizontal error (see Figure 7):

$$err_\beta = \left| \frac{\beta_{eff} - \beta(x_{eff})}{\beta_{eff}} \right|. \tag{17}$$

For GLV dynamics shown above section, the one-dimensional resilience function are $x(\beta_{eff}) = \frac{\alpha}{\beta_{eff}}$ and $\beta(x_{eff}) = \frac{\alpha}{x_{eff}}$, respectively. Therefore, $err_x = err_\beta = \left|1 + \frac{\alpha}{x_{eff}\beta_{eff}}\right|$.

3.4 RANDOM MATRIX APPROACH

In this section, we provide the analytical expression of x_{eff} and β_{eff} when the interaction network A is a random matrix with given different properties.

3.4.1 *Off-diagonal drawn from a bivariate distribution*

In the most general case we consider a matrix **A**, where all pairs of off-diagonal elements - (A_{ij} and A_{ji}) - are drawn from a bivariate distribution with mean μ, standard deviation σ and correlation coefficient ρ and the diagonal elements $A_{ii} = -d_i$ are kept fixed. The distribution from which the elements are drawn is not important, as only mean, variance and correlations are the relevant parameters [23, 25]. Under this setting one can generate both directed and undirected networks, being able to tune also the interaction properties

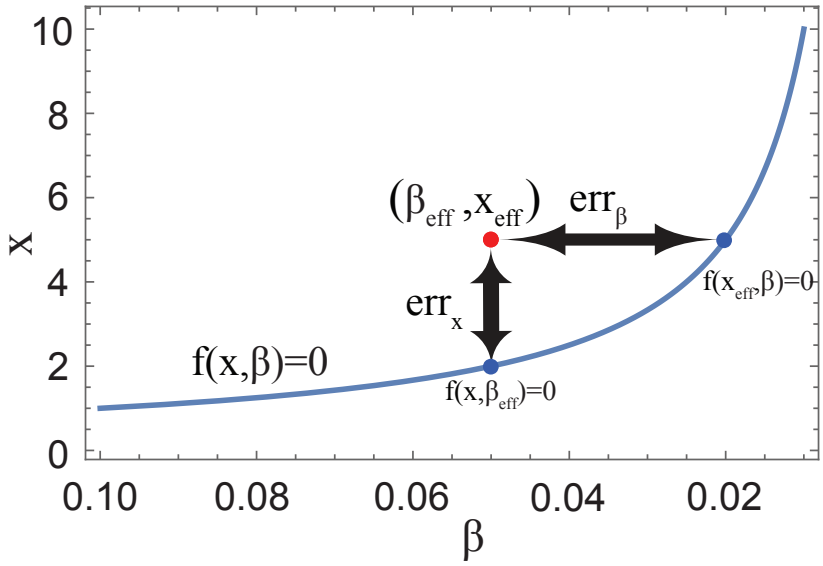

Figure 7: Quantifying the goodness of the one-dimensional system reduction. The red point (β_{eff}, x_{eff}) calculated by Eqs. (6) and (7). The blue curve is the analytical stationary solution of the one-dimensional effective function (8). The vertical and horizontal distances (err_x, err_β) between the points and the curve represent the error of the analytical approximation.

[80]. The following approximate equations would strictly hold only in the very large S: $\mu = \frac{1}{S(S-1)} \sum_{i \neq j} A_{ij}$, $\sigma^2 = \frac{1}{S(S-1)} \sum_{i \neq j} A_{ij}^2 - \mu^2$ and $\rho\sigma^2 = \frac{1}{S(S-1)} \sum_{i \neq j} A_{ij} A_{ji} - \mu^2$ where S is the matrix size. Then one could get the following approximate equations:

$$\sum_{ij} A_{ij} = \sum_{i} A_{ii} + \sum_{i \neq j} A_{ij} = \sum_{i} d_i + S(S-1)\mu$$

$$\begin{aligned}
&\sum_{ijk} A_{ik} A_{kj} \\
&= \sum_{k} \Big(\sum_{i \neq j} A_{ik} A_{kj} + \sum_{i} A_{ik} A_{ki} \Big) \\
&= \sum_{k} \sum_{i \neq j} A_{ik} A_{kj} + \sum_{ki} A_{ik} A_{ki} \\
&= 2 \sum_{i \neq j} A_{ii} A_{ij} + \sum_{i \neq j, j \neq k, k \neq i} A_{ik} A_{kj} + \sum_{i} (A_{ii})^2 + \sum_{i \neq k} A_{ik} A_{ki} \\
&= 2 \Big(\sum_{i} -d_i \Big)(S-1)\mu + S(S-1)(S-2)\mu^2 + \sum_{i} (-d_i)^2 + S(S-1)\rho\sigma^2 + S(S-1)\mu^2 \\
&= \sum_{i} (-d_i)^2 + (S-1) \left[2\mu \sum_{i} (-d_i) + S(S-1)\mu^2 + S\rho\sigma^2 \right]
\end{aligned}$$

For GLV dynamics the analytical solution for the equilibrium state is $\mathbf{x}^* = -\mathbf{A}^{-1} \cdot \boldsymbol{\alpha}$, where $\boldsymbol{\alpha}$ is a vector whose components are all equal

to the constant α, so $\sum_{ij} A_{ij} x_j = -S\alpha$. According to the definition $x_{eff} = \frac{\sum_{ij} A_{ij} x_j}{\sum_{ij} A_{ij}}$ and $\beta_{eff} = \frac{\sum_{ijk} A_{ik} A_{kj}}{\sum_{ij} A_{ij}}$, the following approximations for x_{eff} and β_{eff} are obtained:

$$x_{eff} = \frac{-S\alpha}{\sum_i (-d_i) + S(S-1)\mu} \tag{18}$$

$$\beta_{eff} = \frac{\sum_i (-d_i)^2 + (S-1)\left[2\mu \sum_i (-d_i) + S(S-1)\mu^2 + S\rho\sigma^2\right]}{\sum_i (-d_i) + S(S-1)\mu} \tag{19}$$

3.4.2 *Off-diagonal drawn from a bivariate distribution and diagonal elements set to a constant*

If the diagonal elements of $\mathbf{A}$ are all the same constant ($A_{ii} = -d$ does not depend on i), then Eqs. (18) and (19) become:

$$x_{eff} = \frac{-\alpha}{(-d) + (S-1)\mu} \tag{20}$$

$$\beta_{eff} = \frac{(-d)^2 + (S-1)\left[2\mu(-d) + (S-1)\mu^2 + \rho\sigma^2\right]}{(-d) + (S-1)\mu} \tag{21}$$

3.4.3 *Off-diagonal drawn from a bivariate distribution and diagonal elements drawn from a univariate distribution*

If instead the diagonal elements $A_{ii} = -d_i$ are i.i.d. random variables with given distribution of mean μ_d and standard deviation σ_d, then Eqs. (18) and (19) become:

$$x_{eff} = \frac{-S\alpha}{S\mu_d + S(S-1)\mu} = \frac{-\alpha}{\mu_d + (S-1)\mu} \tag{22}$$

$$\begin{aligned} \beta_{eff} &= \frac{S\left[(\mu_d)^2 + (\sigma_d)^2\right] + (S-1)\left[2\mu S\mu_d + S(S-1)\mu^2 + S\rho\sigma^2\right]}{S\mu_d + S(S-1)\mu} \\ &= \frac{(\mu_d)^2 + (\sigma_d)^2 + (S-1)\left[2\mu\mu_d + (S-1)\mu^2 + \rho\sigma^2\right]}{\mu_d + (S-1)\mu} \end{aligned} \tag{23}$$

3.4.4 *All matrix elements drawn from the same univariate distribution*

Finally, if $\mu = \mu_d$ and $\sigma = \sigma_d$, then $x_{eff} = \frac{-\alpha}{S\mu}$ and $\beta_{eff} = \frac{\mu^2 + \sigma^2 + (S-1)\left[(S+1)\mu^2 + \rho\sigma^2\right]}{S\mu}$. Now the random matrix is generated by i.i.d. random variable ($A_{ij} = p(\mu, \sigma)$) and therefore $\rho \approx 0$. At large S, the following solutions are obtained:

$$x_{eff} = \frac{-\alpha}{S\mu} \tag{24}$$

$$\beta_{eff} \approx \frac{S^2\mu^2 + \sigma^2}{S\mu} \tag{25}$$

3.4.5 *Connectivity*

In the previous analysis, we have set the connectivity (the fraction of non-zero elements) always to one, i.e. $C = 1$. Generalizing the results to not fully connected networks is straightforward. If the mean and standard deviation of the non-zero elements are μ_{dist} and σ_{dist} respectively, then the global mean and standard deviation become $\mu = C\mu_{dist}$ and $\sigma = \sqrt{C\sigma_{dist}^2 + C(1-C)\mu_{dist}^2}$. Substituting the new μ and σ to Eqs. (24) and (25), the new x_{eff} and β_{eff} read:

$$x_{eff} = \frac{-\alpha}{SC\mu_{dist}} \tag{26}$$

$$\beta_{eff} \approx \frac{\left(C\left(S^2-1\right)+1\right)\mu_{dist}^2 + \sigma_{dist}^2}{S\mu_{dist}} \tag{27}$$

3.4.6 *Stability criteria for random matrices*

When dealing with ecological dynamics, we would like to deal with stable fixed points. Therefore, before any perturbations of the system we want to set some bound on the networks parameters so to assure stable and feasible stationary solutions $\mathbf{x}^*$. To do that we can use a random matrix approach. As shown in [25], a feasible fixed point $\mathbf{x}^*$ of the GLV dynamics (i.e. one with all entries $\mathbf{x}_i^* \geqslant 0$) is globally stable if the symmetric interaction matrix $\mathbf{A} + \mathbf{A}^T$ is negative definite. A sufficient condition for this negative definiteness in case of random matrices used in this study is derived in [81]: It can be achieved by setting the diagonal elements to a constant value $A_{ij} = -d$, where d has to be larger than some critical value d_c. In terms of the mean μ, standard deviation σ and correlation coefficient ρ, this critical value is found to be

$$d_c = \begin{cases} (S-1)\mu & \text{if } \mu > 0 \\ \sigma\sqrt{2S(1+\rho)} - \mu & \text{if } \mu \leqslant 0 \end{cases} \tag{28}$$

3.5 ERROR OF THE 1-DIMENSIONAL REDUCTION OF THE MULTI-DIMENSIONAL GLV DYNAMICS

Now we have all elements to quantify the error of the mean field approximation for the analyzed GLV dynamics.

3.5.1 *Error of β_{eff} for any GLV dynamics*

For GLV dynamics, if the random matrix $\mathbf{A}$ is generated by i.i.d. random variable ($A_{ij} = p(\mu, \sigma)$), then $x_{eff} = \frac{-\alpha}{S\mu}$ and $\beta_{eff} \approx \frac{S^2\mu^2+\sigma^2}{S\mu}$

(see Eqs. (24) and (25) in section 3.4.4). According to the definitions of error as distance from the mean point of the numeric realizations (β_{eff}, x_{eff}), Eqs. (16) and (17) in section 3.3, the errors of the framework with respect to the actual quantities measured directly from the network could be predicted quantitatively and given by

$$err_x = err_\beta = \frac{\sigma^2}{S^2\mu^2 + \sigma^2}. \tag{29}$$

Therefore, if the following new condition holds

$$S >> \frac{\sigma}{|\mu|} \tag{30}$$

the collapse will work (i.e. $err_x = err_\beta \approx 0$); Otherwise, the collapse will fail.

Notice that all above conditions hold on average. Fluctuations with respect to the average depends both on connectivity C and size S (see section 3.4.5).

According to Eqs. (29) and (30), the approximation does not work for any positive interaction matrix **A**! On one hand, the new condition, Eq. (30), extends the validity of previous framework for matrix **A** with an asymmetric mixture of positive and negative interactions, as far as the mean μ is not close to zero. The stringent condition on the positive of the interactions is not necessary. On the other hand, if σ is very large with respect to μ and S is not large enough, then the collapse will fail. For example, if interactions strengths are very heterogeneous (e.g. power law distributed), although the interaction is positive (mutualism), the system resilience can not be described by the one-dimensional analytical resilience function.

3.5.2 *Error of β_{eff} for stable GLV dynamics*

We have already seen that depending on the parametrization of the adjacency matrix **A**, Eq. (14) may not have any stable stationary solutions. However, the original work of Gao and collaborators [11] and the above discussion do not consider the existence of a reachable stable point in the multi-dimensional dynamics. Especially for GLV dynamics, the feasibility and stability of Eq. (15) does not imply that the corresponding solution of the full system given by Eq. (14) is feasible and stable. The mean field approximation in this case is not well defined, as x_{eff} can not be actually reached by the corresponding true multidimensional dynamics. Therefore, in order to have a meaningful one-dimensional reduction, the framework should restrict only to matrix **A** that assure stability and feasibility of the complete GLV dynamics .

If the off-diagonal elements of **A** are given by a distribution with mean μ, standard deviation σ and correlation coefficient ρ and the di-

agonal elements are all fixed to a constant ($A_{ii} = -d$), then the effective one dimensional reduction that corresponds to feasible and stable solution of Eq. (14): $x_{eff} = \frac{-\alpha}{(-d)+(S-1)\mu}$ and $\beta_{eff} = \frac{(-d)^2+(S-1)[2\mu(-d)+(S-1)\mu^2+\rho\sigma^2]}{(-d)+(S-1)\mu}$ (see section 3.4.2). For $\mu > 0$, by substituting the case of $\mu > 0$ in Eq. (28) (see section 3.4.6) into Eqs. (20) and (21), the new formulas are $x_{eff} = \frac{-\alpha}{2\mu(S-1)}$ and $\beta_{eff} = \frac{\mu^2(S-1)^2+(S-1)[3\mu^2(S-1)+\rho\sigma^2]}{2\mu(S-1)}$. Finally, by substituting these new formulas of x_{eff} and β_{eff} into Eqs. (16) and (17), the following quantitative estimation of the error could be obtained: $err_x = err_\beta = \left|\frac{\rho\sigma^2}{4(S-1)\mu^2+\rho\sigma^2}\right|$. Therefore, if condition $S >> \frac{|\rho|}{4}\left(\frac{\sigma}{\mu}\right)^2$ holds, then the stationary solution of the GLV dynamics is feasible and stable and the collapse will work (i.e. $err_x = err_\beta \approx 0$). Similarly, for $\mu \leqslant 0$, by substituting the case of $\mu < 0$ in Eq. (28), the final formula is $err_x = err_\beta = \left|\frac{\rho\sigma^2(S-1)}{\mu^2(S-2)^2+2\sqrt{2}\mu\sigma(S-2)\sqrt{(\rho+1)S}+\sigma^2((3\rho+2)S-\rho)}\right|$. The corresponding analytical condition for the success of the approximation is $S >> |\rho|\left(\frac{\sigma}{\mu}\right)^2$. Summarizing the above discussions, the resilience function of the high-dimensional system is well approximated by the one-dimensional resilience function if following condition holds

$$S >> |\rho|\left(\frac{\sigma}{\mu}\right)^2 \tag{31}$$

Eq. (31) highlights that the conditions shown in section 3.1 are neither sufficient nor necessary to guarantee that their method works in general. Indeed, although condition (i) and (ii) are satisfied by the considered GLV dynamics, the new condition poses effective limitations and extensions to the collapse. The quality of the one-dimensional approximation depends on the properties (μ, σ and ρ) of the interaction matrix $\mathbf{A}$, and may hold also for not strictly mutualistic interactions.

Figure 8 shows that the collapse may work for: (A) *Random interaction networks*, where all off-diagonal elements are, with probability C, drawn from a distribution with mean $\mu = 0$ and a given standard deviation σ; (B) *Mutualistic case*, where all off-diagonal elements are, with probability C, drawn from a distribution with positive support as well as (C) *Competitive case*, where all off-diagonal elements are negative or zero. As long as Eq. (31) is satisfied, the approximation works. For small network size the collapse may fail and as the size increases the collapse improves. As expected when $\mu = 0$, independently of the structure of the interaction matrix $\mathbf{A}$ (*Random* or *Predator-Prey*), the collapse fails. Another interesting point evident from Eq. (31) is that for $\rho = 0$ and $\mu \neq 0$, the collapse works independently of the size of $\mathbf{A}$ (see figure 8 D).

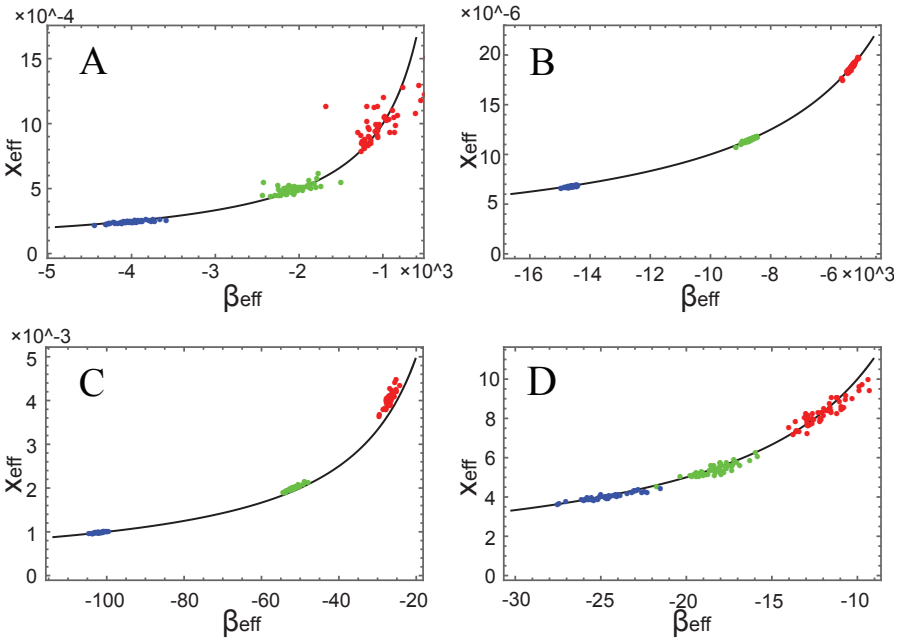

Figure 8: Collapse of the S-dimensional system equations restricted to stable GLV dynamics. Random networks of different sizes 100 (Red), 200 (Green), 400 (Blue) generated by: (A) *Mutualistic case*. A_{ij} are drawn from a Lognormal distribution with mean $\mu = 1$, standard deviation $\sigma = 2.5$ and correlation coefficient $\rho = 0.1$; (B) *Competitive case*. $-A_{ij}$ are drawn from a Lognormal distribution with mean $\mu = 1$, standard deviation $\sigma = 2.5$ and correlation coefficient $\rho = 0.1$; (C) *Random case*. Random networks generated from normal distribution with mean $\mu = 0.5$, standard deviation $\sigma = 1$ and correlation coefficient $\rho = 0.5$. (D) Random networks of different size 50 (Red), 75 (Green), 100 (Blue) generated by normal distribution with mean $\mu = 0.5$, standard deviation $\sigma = 1$ and with correlation coefficient $\rho = 0$.

3.6 BEYOND GLV DYNAMICS

Generalizing previous discussions, especially Eqs. (16) and (17), our results could extend to any model within the class of dynamics considered by Eq. (5). In the most general setting, the stationary solution of Eq. (8) is $\beta(x) = -\frac{F(x)}{G(x,x)}$. Therefore, the following equation holds:

$$err_\beta = \left| 1 + \frac{F(x_{eff})}{\beta_{eff} G(x_{eff}, x_{eff})} \right| \tag{32}$$

For GLV dynamics the key quantity in determining the feasibility of the one-dimensional reduction is a simple function of the product between ρ and σ/μ compared to the system size S. It is possible that this quantity is also crucial in determining the quality of the collapse also for different type of dynamics. If the random matrix $\mathbf{A}$ is generated by i.i.d. random variables ($A_{ij} = p(\mu, \sigma)$) and the new condition given by Eq. (30) holds, then $\beta_{eff} \approx \frac{S^2\mu^2+\sigma^2}{S\mu} \approx S\mu$ does not depend

on the specific dynamics. Therefore, the following equation could be obtained:

$$\mathrm{err}_\beta = \left| 1 + \frac{F(x_{eff})}{S\mu G(x_{eff}, x_{eff})} \right|. \tag{33}$$

It is clear that Eq. (33) goes to zero depends on the functions $F(x_{eff})$ and $G(x_{eff}, x_{eff})$. In other words, the results presented by the original framework hold only for particular choices of $F(x_i)$ and $G(x_i, x_j)$, i.e. those for which $\frac{F(x_{eff})}{S\mu G(x_{eff}, x_{eff})} \approx -1$. In brief, for general dynamics, if the new condition Eq. (30) does not hold, the collapse will fail (e.g. GLV dynamics); if it holds and $\frac{F(x_{eff})}{S\mu G(x_{eff}, x_{eff})} \approx -1$, the collapse will work.

Figure 9 shows the above results by using the dynamics for ecological community given by Eq. 5 in [11], where $B = 0.1, C = 1, K = 5, D = 5, E = 0.9, H = 0.1$. On one hand, the collapse may also work for both positive-negative interactions A_{ij} if S is large enough, exhibited in figure 9 A. On the other hand, Figure 9 B confirms that the conditions shown in section 3.1 are not sufficient to guarantee the validity of the one-dimensional approximation for dynamics beyond GLV. If the standard deviation matrix **A** is very large, the collapse fails also for the specific dynamics.

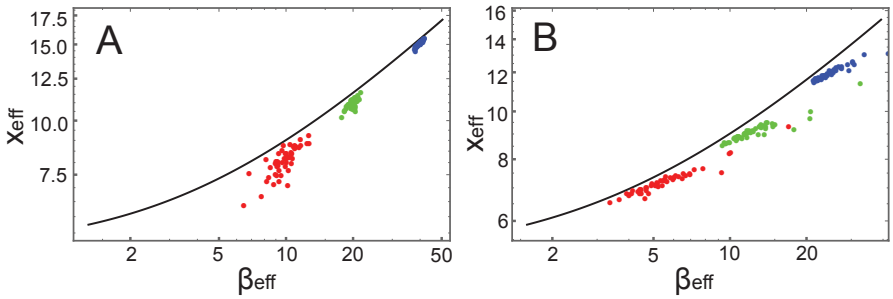

Figure 9: Collapse of the S-dimensional system equations for the non-linear dynamics given by Eq. 5 in [11]. Random networks of different sizes 50 (Red), 100 (Green), 200 (Blue) generated by: (A) *Random case.* Each element of **A** is drawn from a Normal distribution $p(A_{ij}) \sim N(0.2, 1)$. As the size of **A** increases, the collapse improves. (B) *Mutualistic case.* The elements of **A** are drawn from a Lognormal distribution with mean $\mu = 0.096$ and standard deviation $\sigma = 4.253$. When the heterogeneity in the interaction strength is very high ($\sigma \gg \mu$), the collapse fails.

3.7 ERROR AS THE MEAN DISTANCE OF MANY REALIZATIONS OF THE RANDOM SPECIES INTERACTION MATRIX

We can define the error in a more natural way, by considering the mean distance between the mean field approximation and the outcome of different realization of the random species interaction ma-

trix. For each realization of the random matrix, there are two errors (see Figure 7) measuring the vertical and horizontal distance from the point (β_{eff}, x_{eff}) and the stationary solution of the one-dimensional resilience function $x(\beta)$. For the GLV dynamics, both errors become

$$err = \frac{x_{eff} - x(\beta_{eff})}{x_{eff}} = \frac{\beta_{eff} - \beta(x_{eff})}{\beta_{eff}} = 1 + \frac{\alpha}{x_{eff}\beta_{eff}} = 1 - \frac{n}{d} \quad (34)$$

where $n = \sum_{ijkl} A_{ij}A_{kl}$, $d = S \cdot \sum_{ijk} A_{ij}A_{jk}$ and the A_{ij} are the entries of the interaction matrix $\mathbf{A}$.

By taking $\mathbf{A}$ to be a random matrix, the error itself becomes a random variable whose probability distribution is inherited from the distribution of the random matrix. Under the assumption that the means of numerator n and denominator d can be taken independently of each other, the mean and variance could be calculated analytically and are given by:

$$\langle err \rangle = \left\langle 1 - \frac{n}{d} \right\rangle \approx 1 - \frac{\langle n \rangle}{\langle d \rangle} \quad (35)$$

$$\mathrm{Var}(err) = \left\langle \left(\frac{d\langle n \rangle - n\langle d \rangle}{d\langle d \rangle} \right)^2 \right\rangle \approx \frac{\langle d^2 \rangle \langle n \rangle^2 - 2\langle nd \rangle \langle n \rangle \langle d \rangle + \langle n^2 \rangle \langle d \rangle^2}{\langle d^2 \rangle \langle d \rangle^2} \quad (36)$$

The above Eq. (35) and (36) include five terms to calculate

$$\langle d \rangle = S \cdot \left\langle \sum_{ija} A_{ia}A_{aj} \right\rangle ; \quad (37)$$

$$\langle n \rangle = \left\langle \sum_{ijkl} A_{ij}A_{kl} \right\rangle ; \quad (38)$$

$$\langle d^2 \rangle = S^2 \cdot \left\langle \sum_{ijklab} A_{ia}A_{aj}A_{kb}A_{bj} \right\rangle ; \quad (39)$$

$$\langle n \cdot d \rangle = S \cdot \left\langle \sum_{ijklmna} A_{ij}A_{kl}A_{ma}A_{an} \right\rangle ; \quad (40)$$

$$\langle n^2 \rangle = \left\langle \sum_{ijklmnop} A_{ij}A_{kl}A_{mn}A_{op} \right\rangle \quad (41)$$

where all indices are iterated over $\{1, 2, ..., S\}$.

In full generality, we assume that all pairs of off-diagonal elements (A_{ij} and A_{ji}) are drawn from a bivariate distribution with mean μ, standard deviation σ and correlation coefficient ρ. The diagonal elements are either drawn from a univariate distribution following the same statistics as the off-diagonal elements or kept fixed and constant by setting $A_{ii} = -d_i$. The analytical derivation is complicated

and tedious. Even in the simplest version of random matrix A, the entries A_{ij} are all i.i.d., the pairs A_{ij}^2 need to be separate out, because they will lead to contributions other than μ^2 where $\mu = \langle A_{ij} \rangle$ (and similarly for higher order tuples). In order to do so, we devised an algorithm to solve it.

3.7.1 *Results*

The analytical formula of mean and variance of the error for different cases of interaction matrices A at the highest order in the network size S are listed in table 1.

Case	$\langle err \rangle$	$\mathrm{Var}(err)$
A_{ij} i.i.d.	0 (exact)	$\frac{\sigma^4}{S^3\mu^4}$
Correlation ($\rho = 0$):		
$\rho = \mathrm{corr}(A_{ij}, A_{ji}) \in [-1, 1]$	$\frac{\rho\sigma^2}{S\mu^2}$	$\frac{\sigma^4}{S^3\mu^4}\left(2\frac{\mu^2}{\sigma^2}\rho + (\rho-1)^2\right)$
Constant diagonal:		
$A_{ii} = -d$ of order 1 or $\sqrt{S}$	$\frac{\sigma^2((S-2)\rho-1)}{S^2\mu^2}$	$\frac{\sigma^4}{S^3\mu^4}\left(2\frac{\mu^2}{\sigma^2}\rho + (\rho-1)^2\right)$
for $\rho = 0$	$-\frac{\sigma^2}{S^2\mu^2}$	$\frac{\sigma^4}{S^3\mu^4}$
for $\rho \neq 0$ and $S \gg 1$	$\frac{\sigma^2\rho}{S\mu^2}$	$\frac{\sigma^4}{S^3\mu^4}\left(2\frac{\mu^2}{\sigma^2}\rho + (\rho-1)^2\right)$
$A_{ii} = -d$ of order S	$\frac{\sigma^2((S-2)\rho-1)}{S^2\mu^2\left(\frac{d}{d_c}-1\right)^2}$	$\frac{\sigma^4}{S^3\mu^4\left(\frac{d}{d_c}-1\right)^4}\left(2\frac{\mu^2}{\sigma^2}\rho + (\rho-1)^2\right)$
for $\rho = 0$ and $S \gg 1$	$-\frac{\sigma^2}{S^2\mu^2\left(\frac{d}{d_c}-1\right)^2}$	$\frac{\sigma^4}{S^3\mu^4\left(\frac{d}{d_c}-1\right)^4}$
for $\rho \neq 0$ and $S \gg 1$	$\frac{\sigma^2\rho}{S\mu^2\left(\frac{d}{d_c}-1\right)^2}$	$\frac{\sigma^4}{S^3\mu^4\left(\frac{d}{d_c}-1\right)^4}\left(2\frac{\mu^2}{\sigma^2}\rho + (\rho-1)^2\right)$

Table 1: Analytical formulas approximating to highest order in S

The results in Table 1 can be summarized as follow: :

- In all cases, the error (or its fluctuations) grows without bound if the ratio $\frac{\mu}{\sigma}$ goes to zero for a given network size S.
- The order of the fluctuations (namely $S^{-\frac{3}{2}}$) remains the same for all cases, while the order of the mean changes. In particular, for interaction matrices A without correlation ($\rho = 0$), the term dominating the error for large S are the fluctuations while the mean value is either zero (for i.i.d. entries A_{ij}) or of order S^{-2} (in case of a constant diagonal). On the other hand, for networks with non-zero correlation, the mean becomes the dominating term of order S^{-1}.
- If the diagonal is of the same scale as S, the error may explode. This happens if $A_{ii} = -d_c$, where $d_c = (S-1)\mu$ corresponds to the value of d where the interaction matrix becomes stable and non-reactive for positive μ.

Similar as the results of the first definition, the collapse does not work for any positive interaction matrix $\mathbf{A}$. On one hand, the new condition extends the validity for matrix $\mathbf{A}$ with an asymmetric mixture of positive and negative interactions, as far as the mean μ is not close to zero. On the other hand, if the standard deviation of matrix $\mathbf{A}$ is very large with respect to the mean μ and the size S is not large enough, then the collapse will fail.

In order to test these analytical results, the interaction matrix with the corresponding statistics numerically are sampled and compared to the empirical mean and standard deviation with the theoretical predictions. The results can be observed in figure 10. In all cases, the theoretical predictions are met very well. There is a notable but small deviation for small network size $S = 20$, namely slight underestimation of the mean for the case of correlation, for example plot B of figure 10.

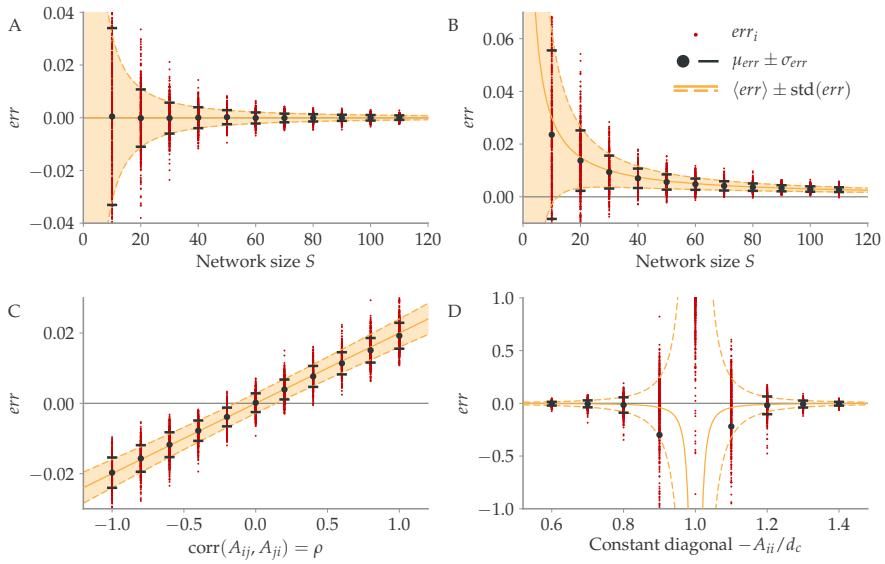

Figure 10: Comparison of theoretical results with numerical samples. Each red dot corresponds to the error calculated for one interaction matrix. For each case, 500 matrices are sampled independently and calculated empirical means μ_{err} and standard deviations σ_{err} (plotted as black dots and bars, respectively). The theoretical mean $\langle err \rangle$ is plotted as an orange line, the shaded area indicates the predicted standard deviation std(err). For all figures, the entries of $\mathbf{A}$ are drawn from a normal distribution with $\mu = \sigma = 1$. The upper plots show the effect network size on the error in the case of (A) all elements drawn i.i.d. or (B) with positive correlation $\rho = 0.3$. The lower plots show the error for networks of size $S = 50$ for (C) varying correlation ρ or (D) enforcing a constant diagonal A_{ii} relative to the critical value d_c.

Similar as section 3.5.2, by combining the formulas of this new definition with the D-stability, the analysis could still be restricted only to the random matrix A that assure stability and feasiblity of the com-

plete GLV dynamics. According to Eq. (28), for $\mu \leqslant 0$, the critical value to have stable GLV dynamics is $d_c = \sigma\sqrt{2S(1+\rho)} - \mu$ (that is d of order $\sqrt{S}$ - rows 5-7 in table 1). For $\mu > 0$, stable GLV dynamics are assured if $d_c = (S-1)\mu$, that is d of order S (rows 8-10 in Table 1). Note that for the case of a constant diagonal close to the critical value, shown in Figure 10 (D), the theoretical value is not expected to give a good approximation to the empirical average, since in this case, the expected value of the denominator $\langle d \rangle$ becomes zero. In this case, the approximation of taking numerator and denominator separately is not justified. Furthermore, sampling becomes difficult, as outliers may govern the empirical mean and standard deviation.

3.8 CONCLUSIONS

In this chapter, we have studied under which condition a large dynamical system can be effectively approximated with one-dimensional equation. We have adopted two different definitions to quantify the error. The order parameter that appears as a variable in the effective equation can be obtained from a simple expression of the local variables using an approach based on random matrix. Under this approximation, it becomes clear which properties of the interactions determine the state of the system and it turns out to be possible to quantify their effects.

We have then explored which properties of the interactions determine the accuracy of the approximation. In general, the form of the multi-dimensional equations and how the non-linearities in the dynamics are introduced, will influence the opportunity to approximate the original set of equations with the corresponding one-dimensional mean field equation. In order to focus on the effect of the interactions, we therefore first have considered a simple idealized scenario, the generalized Lotka-Volterra equations, where the interactions are linear. In this context, the accuracy of the approximation is only determined by the interaction matrix.

The criterion we have obtained relates the variability of the interactions between the agents/nodes and its number. In particular, for the approximation to work, the size of the system has to be larger than a critical value proportional to the coefficient of variation of the interaction strengths. Additionally, the reciprocity of interactions plays an important role: the approximation is expected to work for any interaction strengths if there is not any correlation in the activity between each pair of nodes in the network. As the correlation between reciprocal interactions is increased, the larger the size of the system must be, so to guarantee the accuracy of the approximation.

Finally, we have shown that the approximation works also for interaction matrices with a mixture of positive and negative signs and that it can be extended to more complicated and non-linear dynamics.

These results open up possible applications of the mean-field framework to food-webs, neuronal networks and social/economic interactions.

Part II

COOPERATION PROMOTES BIODIVERSITY AND STABILITY

On the basis of biological, sociological, and historical knowledge, we should recognize that the individual self is subject to death or decay, but the sum total of individual achievement, for better or worse, lives on in the immortality of The Larger.

— Hu Shih (1891 - 1962)

4

NEUTRAL THEORY AND BEYOND

He who learns but does not think, is lost. He who thinks but does not learn is in great danger.

— Confucius (551 BC - 479 BC)

4.1 BACKGROUND

Research in population dynamics has a long history dating back to almost one thousand year ago with Fibonacci modeling of rabbits population. Nevertheless, there are still several open issues of paramount importance in the research of ecological population dynamics [82, 83, 84, 85, 86, 87] and the current loss of earth biodiversity [88, 89] makes this research field of great relevance today more than ever. Many fundamental and long-standing questions in biology concerning ecosystem dynamics are, for example, how does simplicity result from apparently complex interactions? How does diversity emerge and what is the role of cooperation? How are these features maintained through robust mechanisms? When several species co-occur in a community there can be a rich set of relationships among them that can be represented as a complex interaction network. Historically, the first models defining the dynamics of interacting ecological species were those of Lotka [90] and Volterra [91], which describe asymmetrical interactions between predator-prey or resource-consumers systems. The Lotka and Volterra (LV) equations have provided much theoretical guidance [92, 93, 94] and translated in mathematical terms the modelling of population dynamics based on a "niche" point of view.

Niche theories put the emphasis on phenotypic differences and state that formation of coexisting species is only possible through diversification for exploitation of the resources, minimizing competition among individuals, and postulates that the number of coexisting species is equal to the number of niches or ways to exploit the resources of the environment (this is what has been called the niche dimension hypothesis [95, 96, 97, 98]).

While prey-predator and competitive interactions have been extensively studied, mutualistic/commensalistic interactions, which are beneficial to the involved species - see Fig. 6 - have historically received less attention. Nevertheless, in recent years, there have been several studies showing the crucial role of cooperation in ecosystems [7, 67, 69, 99, 70]. Therefore the question is how mutualistic interactions affect and or change the niche dimension hypothesis.

Indeed, one of the fundamental problems in theoretical ecology is the search for key mechanisms leading to the emergence and coexistence of biodiversity [70, 100, 101, 7]; a deep understanding of the underlying dynamics becomes essential for the maintenance and conservation of natural ecosystems. In most of the cases, experiments in vivo are not always possible, and the only reliable procedure is the use of mathematical descriptions combined with experimental data.

The current approach study to mutualistic/commensalistic population dynamics is the same one as in the LV models, but with beneficial interactions among individuals of different species [83, 102, 47]. The limitations of these approaches were identified as more research was carried out. Indeed, a generalization of the May stability-complexity theorem [47, 45] has revealed that mutualism and cooperation in LV models are more detrimental to stability than predator-prey interactions as the product SC increases [23, 24, 7, 49], where S is the number of species and C, the connectivity, is the fraction of non-zero pairwise interactions between species.

4.2 THE COMPLEXITY-STABILITY PARADOX: A RANDOM MATRIX PERSPECTIVE

In the last years, many works [23, 24, 80, 103, 104, 105] have investigated the relationship between stability and the role of different interaction types by using analytical results based on Random Matrix Theory (RMT).

4.2.1 *May's complexity-stability paradox*

Forty years ago, May [32, 47] showed that a sufficiently large ecological network resting at a feasible equilibrium point would invariably be unstable: arbitrarily small perturbations of the population densities would drive the system away from equilibrium. Assuming that the ecological community composed of S populations is a continuous-time dynamical system, the following ordinary differential equations hold

$$\frac{dX_i(t)}{dt} = f_i(\mathbf{X}(t)), \quad i = 1, ..., S \tag{42}$$

where $X_i(t)$ represents the density of population i at time t, the vector $\mathbf{X}(t)$ is the population densities and f_i is a function relating the growth rate of population i to the density of the S populations. The system is at an equilibrium point $\mathbf{X}^*$ whenever

$$\frac{dX_i(t)}{dt}|_{X^*} = f_i(\mathbf{X}^*) = 0 \tag{43}$$

The equilibrium is said to be locally stable if all infinitesimal perturbations die out eventually and its analysis is carried out by linearization

of the system at the equilibrium point. By substituting the densities of the populations $\mathbf{X}(t)$ into its Jacobian matrix $J_{ij}(\mathbf{X}) = \frac{\partial f_i \mathbf{X}(t)}{\partial X_j}$, its community-matrix $\mathbf{M}$ is given by:

$$M_{ij} = J_{ij}|\mathbf{X}^* = \frac{\partial f_i \mathbf{X}(t)}{\partial X_j}|\mathbf{X}^* \tag{44}$$

Each equilibrium corresponds to a community matrix and its coefficient M_{ij} measures the effect of a slight increase in the population j on the growth rate of population i. If all eigenvalues have negative real parts, then the equilibrium is stable. May's insight [106, 47] was to skip the Jacobian matrix altogether, to consider directly the community matrix, modeled as a large random matrix, and to attempt estimating the real part of the "rightmost" eigenvalue based on the characteristics of the random matrix.

4.2.2 *Random matrix perspective*

Allseina et al. [23] extend May's results to real spices interactions, for example predator-prey, mutualistic or competitive, and find remarkable differences between predator-prey interactions, which are stabilizing, and mutualistic and competitive interactions, which are destabilizing. For a random matrix $\mathbf{M}$ whose entries are independently sampled from a statistical distribution, the following five quantities are essential for determining the largest real part of its eigenvalues [23, 81]:

1. the dimension of $\mathbf{M}$, S, describing the number of species in the network
2. the expectation of the off-diagonal entries, $E = \langle (M_{ij})_{i \neq j} \rangle$, describing the inter-specific interaction strengths
3. the expectation of the diagonal entries, $-d = \langle M_{ii} \rangle$, describing the intra-specific interaction strengths
4. the variance of the off-diagonal entries, $V = Var(M_{ij})_{i \neq j} \geqslant 0$
5. the pairwise interaction correlation, $\rho = \frac{\langle M_{ij} M_{ji} \rangle_{i \neq j} - E^2}{V}$

Allseina et al. [23] showed that there is always one eigenvalue of $\mathbf{M}$ (denoted by $\lambda_R^{\mathbf{M}}$) whose real part is close to the expected row sum of $\mathbf{M}$:

$$\Re(\lambda_R^{\mathbf{M}}) \approx (S-1)E - d \tag{45}$$

When S is sufficiently large, the other $(S-1)$ eigenvalues of $\mathbf{M}$ are approximately uniformly distributed on an ellipse centered at $(-E-d, 0)$, whose horizontal and vertical axes are about $2\sqrt{SV}(1+\rho)$ and $2\sqrt{SV}(1-\rho)$, respectively. Therefore, the right most one of these $(S-$

1) eigenvalues (denoted by $\Re(\lambda^{\mathbf{M}}_{EL})$) can be estimated using the "center" plus the semi-length of the horizontal axis:

$$\Re(\lambda^{\mathbf{M}}_{EL}) \approx -E - d + \sqrt{SV}(1+\rho) \tag{46}$$

Finally, the stability criteria [81] is

- $E > 0, (S-1)E < d$
- $E \leqslant 0, \sqrt{SV}(1+\rho) - E < d$

Allseina et al. [23] applied the above criteria to separate the contribution of network structure and interaction strengths to stability as well as found

1. The probability of stability for predator-prey networks decreases when a realistic food web structure is imposed or if there is a large preponderance of weak interactions.
2. Stability is negatively affected by nestedness in bipartite mutualistic networks.
3. Stable predator-prey networks can be arbitrarily large and complex, provided that predator-prey pairs are tightly coupled.

4.3 NEUTRAL THEORY OF BIODIVERSITY AND BEYOND

From a theoretical point of view, an alternative approach to niche-based multi-species deterministic modeling is the Neutral Theory (NT) of Biodiversity [82, 107, 108, 109, 110, 111, 84, 112]. The NT is an ecological theory within which organisms of a community have identical per-capita probabilities of giving birth, dying, migrating, and speciating, regardless of the species they belong to. In this sense the model is symmetric and it aims to model only species on the same trophic level-species therefore competing for the same pool of resources. For instance, plants and trees in a forest compete for resources like carbon, nitrate and light.

Hubbell [82] generalized this neutral theory to explore the expected steady-state distribution of relative species abundance (RSA) in the local community under restricted immigration. Volkov et al. [108] presented a theoretical framework for the unified neutral theory of biodiversity and an analytical solution for the distribution of the RSA both in the metacommunity and in the local community. Assuming that

- $b_{n,k}$ represents the probability of birth in the k-th species with n individuals and $b_{-1,k} = 0$
- $d_{n,k}$ represents the probability of death in the k-th species with n individuals and $d_{0,k} = 0$

- $p_{n,k}(t)$ represents the probability that the k-th species contains n individuals at time t

The time evolution of $p_{n,k}(t)$ is regulated by the master equation [113, 114]:

$$\frac{dp_{n,k}(t)}{dt} = p_{n+1,k}(t)d_{n+1,k} + p_{n-1,k}(t)b_{n-1,k} - p_{n,k}(t)(b_{n,k} + d_{n,k}) \tag{47}$$

whose equilibrium solution is

$$P_{n,k} = P_{0,k} \prod_{i=0}^{n-1} \frac{b_{i,k}}{d_{i+1,k}} \tag{48}$$

where $n > 0$ and $P_{0,k}$ can be deduced from the normalization condition $\sum_n P_{n,k} = 1$.

The frequency of species containing n individuals is given by

$$\phi_n = \sum_{k=1}^{S} I_k \tag{49}$$

where S is the total number of species and I_k is a random variable which takes the value 1 with probability $P_{n,k}$ and 0 with probability $(1 - P_{n,k})$. Its average number is

$$\langle \phi_n \rangle = \sum_{k=1}^{S} P_{n,k} \tag{50}$$

4.3.1 *RSA of metacommunity*

If the species in a metacommunity are demographically identical and density independent, i.e. $b_{n,k} = b_n = bn$ and $d_{n,k} = d_n = dn$, the following equation will hold

$$\left\langle \phi_n^M \right\rangle = SP_0 \prod_{i=0}^{n-1} \frac{b_i}{d_{i+1}} = S_M P_0 \frac{b_0 b_1 ... b_{n-1}}{d_1 d_2 ... d_n} = \phi \frac{x^n}{n} \tag{51}$$

where M refers to the metacommunity, $x = b/d$ represents the ratio of effective per capita birth rate to the death rate arising from a variety of causes and $\theta = S_M P_0 \nu / b$ is the biodiversity parameter.

4.3.2 *RSA of local community*

If a local community of size J is semi-isolated from the surrounding metacommunity, one may introduce an immigration rate m and the dynamical rules [82, 115] governing the stochastic processes in the community are:

- With probability $1-m$, pick two individuals at random from the local community. If they belong to the same species, no action is taken. Otherwise, with equal probability, replace one of the individuals with the offspring of the other
- With probability m, pick one individual at random from the local community. Replace it by a new individual chosen with a probability proportional to the abundance of its species in the metacommunity.

The above rules lead to the following expressions for effective birth and death rates for the k-th species

$$b_{n,k} = (1-m)\frac{n}{J}\frac{J-n}{J-1} + m\frac{\mu_k}{J_k}\left(1-\frac{n}{J}\right) \tag{52}$$

$$d_{n,k} = (1-m)\frac{n}{J}\frac{J-n}{J-1} + m\left(1-\frac{\mu_k}{J_k}\right)\frac{n}{J} \tag{53}$$

where μ_k is the abundance of the k-th species in the metacommunity and J_M is the total population of the metacommunity.

Substituting above equations into Eq. 48, one obtains the expression

$$P_{n,k} = \frac{J!}{n!(J-n)!}\frac{\Gamma(n+\lambda_k)}{\Gamma(\lambda_k)}\frac{\Gamma(\nu_k-n)}{\Gamma(\nu_k-J)}\frac{\Gamma(\lambda_k+\nu_k-J)}{\Gamma(\lambda_k+\nu_k)} \equiv F(\mu_k) \tag{54}$$

where $\lambda_k = \frac{m}{1-m}(J-1)\frac{\mu_k}{J_m}$ and $\nu_k = J + \frac{m}{1-m}(J-1)(1-\frac{\mu_k}{J_M})$. By substituting above equation into Eq. 50, one obtains:

$$\langle \phi_n \rangle = \sum_{k=1}^{S_M} F(\mu_k) = S_M \langle F(\mu_k) \rangle = S_M \int d\mu \hat{\rho}(\mu) F(\mu) \tag{55}$$

where $\hat{\rho} d\mu = \frac{1}{\Gamma(\epsilon)\sigma^\epsilon} exp(-\mu/\sigma)\mu^{\epsilon-1} d\mu$ is the probability distribution of the mean populations of the species in the metacommunity. Taking the limits $S_M \to \infty$ and $\epsilon \to 0$ with $\theta = S_M \epsilon$ approaching a finite value [115] and on defining $y = \mu\frac{\gamma}{\sigma\theta}$, one can obtain the analytic expression of the local community

$$\langle \phi_n \rangle = \theta \frac{J!}{n!(J-n)!}\frac{\Gamma(\gamma)}{\Gamma(J+\gamma)}\int_0^\gamma \frac{\Gamma(n+y)}{\Gamma(1+y)}\frac{\Gamma(J-n+\gamma-y)}{\gamma-y} exp(-y\theta/\gamma) dy \tag{56}$$

where $\Gamma(z) = \int_0^\infty t^{z-1}e^{-t}dt$ and $\gamma(z) = \frac{m(J-1)}{1-m}$.

4.3.3 *Voter model*

Another important example of neutral model is the Voter Model (VM) [51, 52, 116, 117, 53]. The VM is a paradigmatic model to describe

competition in many fields going from social sciences [118] to biology [119]. In the ecological context one deals with a community of N individuals belonging to S different species. At every time step a randomly selected individual dies and the corresponding resources are freed up for colonization.

- With the probability ν the site is taken by an individual of a species not currently present in the system (immigration from surrounding communities or speciation event)
- With the probability $1-\nu$ the available site is colonized by an individual randomly sampled within the community [111, 84]

However, an important limitation of this modeling is that it does support species coexistence without speciation (e.g. for $\nu = 0$) and it does not consider explicitly species interactions (e.g. mutualism/-commensalism). Moreover, adding mutualisitic interactions typically places a bound on the diversity of species that can coexist [23, 7, 24, 49]. Two crucial gaps in the current literature are thus:

1. a general framework where species interactions are added on neutral models [82, 108, 84] and can modify the species birth-death rates
2. understand the role of mutualistic/commensalistic interactions in determining species coexistence also in the limit $\nu = 0$ and how they impact on patterns such as species abundance distribution [84]

In the next chapter, we present a theoretical framework, where starting from a VM-like microscopic stochastic modeling, we add mutualistic/commensalistic interactions among species, affecting neutrality and leading to an emergent niche-like multi species-mutualistic model. Reconciling apparently contrasting observations and previous results [47, 45, 23, 7, 49], we show that in our model ecosystem cooperation promotes biodiversity and diversity increases its stability.

5 THE COOPERATIVE VOTER MODEL

When you know a thing, to hold that you know it, and when you do not know a thing, to allow that you do not know it - this is knowledge.

— Confucius (551 BC - 479 BC)

We now present a general framework where mutualistic species interactions are added on neutral models [83, 24, 7] and modify the species birth rates. In this way we can investigate the role of mutualistic/commensalistic interactions in determining species coexistence and how they impact on the ecosystem stability and patterns such as species abundance distribution.

5.1 A VOTER MODEL WITH MUTUALISTIC INTERACTIONS

Assuming that η_x is the species label at spatial position x where $\eta_x \in \{1,\dots,S\}$ and $x = 1,\dots,N$, the state at time t of the system is given by $\eta(t) = (\eta_1(t),\eta_2(t),\dots,\eta_N(t))$. We introduce a directed graph on the set $\{1,\dots,S\}$, where the nodes correspond to species and directed links represent the network of ecological interactions. Given two species i and j, a directed link of strength M_{ij} from i to j means that the i-th species interacts with the j-th species. If $M_{ij} > 0$, then the presence of the i-th species helps the j-th species to survive, i.e. we have cooperation. In our model, we focus on mutualistic interactions, $M_{ij} > 0,\ M_{ji} > 0$ (reciprocal cooperation), and commensalistic interactions, $M_{ij} > 0,\ M_{ji} = 0$ or $M_{ij} = 0,\ M_{ji} > 0$, where only one species benefices of the presence of the other one.

Using a random matrix approach, the matrix entries can be drawn from a given probability distribution [23, 25] and they are decided at time $t = 0$ and do not change with dynamics (quenched dynamics). With the matrix M in hand, we can describe the Markovian dynamics for the time evolution of $\eta(t)$ in terms of the transition rates between states.

We define the fraction of individuals of the k-species as $\bar{\eta}^k = \sum_x \delta_{\eta_x,k}/N$ where δ is Dirac delta function. In the dynamics, a random individual is eliminated and the freed space is colonized by an individual of given species j with a rate

$$\omega(j,\eta,M) = \bar{\eta}^j + \epsilon \sum_{k=1}^{S} \bar{\eta}^k M_{kj} \theta(\bar{\eta}^j) \tag{57}$$

where ϵ gives the cooperation intensity, so that we can fix the average of the non-zero M_{kj}'s to 1, and $\theta(\cdot)$ is the Heaviside step function, i.e.,

$\theta(x) > 0$ when $x > 0$ and 0 otherwise. The presence of the θ-function guarantees that the transition rate is zero if the j-th species is extinct.

- When $\epsilon = 0$, we recover the standard VM
- When $\epsilon > 0$, the species j is favored by the presence of the other species (k in the summation) to which it is connected and by their population

We have presented the model by neglecting spatial effect on ecosystems dynamics. Adding spatial interactions in this framework is not complicated from a numerical point of view (we just restrict competition over space colonization only to neighbours individual), but we loose all analytical results.

It is useful to highlight the differences between the form of the interaction part in our rates (last term of Eq. (57)), with the corresponding one in the LV equations. In the LV equation for the time evolution of the population of the j-th species, the interaction term would read $\sum_{k=1}^{S} \bar{\eta}^k B_{kj} \bar{\eta}^j$. Similarly, to M in (57), the matrix B describes the interaction among species and B_{kj} is positive (negative) if j is the predator (prey) and k is the prey (predator). The main difference is that this interaction term is quadratic in $\bar{\eta}$, while in our setting it is linear.

Indeed, we are stressing that mutualism and predator-prey interactions are interactions types of different nature. In predator prey, this term describes the probability that two species interact (which would proportional to the product of the abundance of both the species like it would happen in a chemical reaction between two reactants). On the other hand we conceptualize this term by expressing a biological links among species, and focus on their impact on the birth rates $\omega(j, \eta, M)$. The interaction $M_{i,j} > 0$, as we have written, corresponds to the case where species i helps species j to survives. This may happen in a bacterial community where the presence of certain species create a friendly environment for other species to live in. Thus this environment is there independently of the population of the j-th species. A simple example where this claim can be proved is the following, inspired by a recent contribution by [120]. Let c be the concentration of a given resource used by the species j. This resource is provided, at a rate s, by certain species and related to their populations in a linear way, that is $s = \sum_k \eta_k M_{kj}$. The kinetic of nutrient concentration is thus

$$dc(t)/dt = s - \eta_j(t) r(c(t)), \tag{58}$$

where $r(c)$ is the consumption rate per individual whose specific form is irrelevant as fas as it has the qualitative feature of the Monod function $r(c) = \alpha c/(K + c)$, with α and K some suitable constants. The contribution to the growth rate of the j-th species, due to this nutrient,

is $\delta\omega = \epsilon r(c)\eta_j$, where ϵ is a conversion factor measuring how the nutrient contributes to the biomass of the j-th species. If the nutrient concentration is in quasi-steady state, that is $dc(t)/dt = 0$, which occurs if it relaxes much faster than populations, then, from the above equation, we get $r(c(t)) = s/\eta_j(t)$, leading to $\delta\omega = \epsilon s = \epsilon \sum_k \eta_k M_{kj}$ if $\eta_j > 0$. This is why we have assumed in Eq. (57) the interaction term to be linear.

5.2 MEAN-FIELD ANALYSIS FOR THE MODEL

We now want to characterize the large size limit of the dynamics described above. The microscopic dynamics given by rates (57) induce a Markovian evolution on the relative abundance $\bar{\eta}^s$ of each species. Standard techniques of convergence of generators [121] can be used to prove that as $N \to \infty$, the process $(\bar{\eta}^1(t), \dots, \bar{\eta}^S(t))_{t \geqslant 0}$ weakly converges to the solution of the system of ordinary differential (mean field) equation:

$$\frac{d}{dt}\bar{\eta}^s = \epsilon \sum_{k=1}^{S} \bar{\eta}^k M_{ks}\, \theta(\bar{\eta}^s) - \epsilon\, \bar{\eta}^s \sum_{i,j=1}^{S} \bar{\eta}^i M_{ij}\, \theta(\bar{\eta}^j) \tag{59}$$

where $s = 1, \dots, S$ represents different species, $\bar{\eta}^s$ is the fraction of individuals of the s-species, M represents the network of ecological interaction, θ is the Heaviside step function and ϵ is the cooperation intensity. For simplicity, we have omitted in the notation in the time dependence.

We have also studied the same model where we relaxed the zero-sum hypothesis introducing the possibility for a site to become empty at rate $\lambda < 1$. If empty site are assigned to the 0-th species we still have $\sum_{j=0}^{S} \bar{\eta}^j(t) = 1$ at all times, whereas $\sum_{j=1}^{S} \bar{\eta}^j(t) \leqslant 1$ and its stationary value will depend on λ, i.e. a soft constraint on the average population in the community is implemented by introducing a non-zero λ. All presented results do not change when empty sites are considered: all stationary populations are simply rescaled by a global multiplicative factor which depends on λ. We will show below that, under suitable hypothesis, a stationary solution of Eq. (59) exists and it will be denoted $m_j = \lim_{t\to\infty} \bar{\eta}^j(t)$.

5.2.1 *Voter model with empty sites*

We now extend the model presented in the main text introducing the possibility for a site to be empty, i.e. relaxing the zero-sum constraint. In our setting, empty sites do not interact with species and thus their birth rates remain unchanged after the introduction of empty sites. Non-empty sites become empty with rate λ. In the case $\epsilon = 0$, the rate λ has to be less than 1 otherwise empty sites will cover all the

available space. If we denote with $\bar{\eta}^0_t$ the number of empty sites at time t, then the mean field equations, obtained with similar computations as Eq. (59) and read

$$\begin{cases} \frac{d}{dt}\bar{\eta}^s = \bar{\eta}^s\bar{\eta}^0 - \bar{\eta}^s\lambda + \epsilon \sum_{k=1}^{S} \bar{\eta}^k M_{ks}\, \theta(\bar{\eta}^s) - \epsilon\, \bar{\eta}^s \sum_{i,j=1}^{S} \bar{\eta}^i M_{ij}\, \theta(\bar{\eta}^j) \\ \frac{d}{dt}\bar{\eta}^0 = (1-\bar{\eta}^0)(\lambda - \bar{\eta}^0) - \epsilon\, \bar{\eta}^0 \sum_{i,j=1}^{S} \bar{\eta}^i M_{ij}\, \theta(\bar{\eta}^j) \end{cases} \tag{60}$$

Let us analyze the mean-field equations for $\epsilon << 1$. In this case the stable equilibrium for the empty sites is $\bar{\eta}^0 = \lambda - \epsilon \frac{\lambda}{1-\lambda} \sum_{i,j=1}^{S} \bar{\eta}^i M_{ij}\, \theta(\bar{\eta}^j) + O(\epsilon^2)$. Substituting in the equations for $\bar{\eta}^s$, we obtain

$$\frac{d}{dt}\bar{\eta}^s = \epsilon \sum_{k=1}^{S} \bar{\eta}^k M_{ks}\, \theta(\bar{\eta}^s) - \epsilon \left(\frac{1}{1-\lambda}\right) \bar{\eta}^s \sum_{i,j=1}^{S} \bar{\eta}^i M_{ij}\, \theta(\bar{\eta}^j) + O(\epsilon^2) \tag{61}$$

where $s = 1, \ldots, S$. After the change of variable $\bar{\eta}' = (1-\lambda)\bar{\eta}$, the above Eq. (61) reduces to the Eq. (59) up to a second order perturbation in ϵ. In other words, when ϵ is small, the introduction of empty sites does not change a lot the dynamics of the species. The time evolution remains $O(\epsilon^2)$ close to the one described by (59) but on "smaller" ecosystem as a λ fraction of the space is occupied by empty sites.

An intuitive path to Eqs. (59) and (60) can be as follows. For large N the evolution of the quantity $\bar{\eta}^s_N$ becomes deterministic because the noise is canceled in the macroscopic regime and in the thermodynamics limit the relative abundance converges to its mean. Then, observe that the dynamics of the relative abundance in the infinitesimal time dt is simple as it can only decrease by $1/N$ when a site of kind s change type or can increase by $1/N$ when the new symbol of a certain site is s. The same argument holds for $\bar{\eta}^0$.

5.3 ANALYTIC SOLUTION OF THE MEAN-FIELD EQUATION

If M is non negative and irreducible, i.e. if for any node i we can reach any other node j through a path of oriented links (k, l) such that $M_{kl} > 0$, then the Perron-Frobenius (PF) theorem holds [122] and a non-trivial stationary state, $(m_k)_{k=1,\ldots,S}$, exists with all positive entries and it is unique. It is proportional to the left eigenvector, ν, of M corresponding to the eigenvalue of M with the largest modulus, which turns out to be non-degenerate, positive and will be denoted α in the following. All components of ν are strictly positive and so $m_i = \nu_i / \sum_k \nu_k$. An example of irreducible matrix M occurs when

$M_{ij} > 0$ implies $M_{ji} > 0$ and the network has a single connected component.

Let m_i with $i = 1, \ldots, S$ the stationary solution of equation (59). If all the components are positive, they are solutions of

$$\sum_k m_k M_{ki} = m_i \sum_{jk} m_k M_{kj} \tag{62}$$

If M is irreducible, which means to require that a path of oriented links (a link is present from i to j is $M_{ij} > 0$) exists joining each pairs of nodes, say k and l, then the Perron-Frobenius theorem holds (see Theorem 1.5 in [122]). In this case a positive solution, i.e. $m_k > 0$ for all k, exists, it is unique and it is proportional to the left eigenvector, v, of M corresponding to the eigenvalue of M with the largest real part (see Theorem 1.7 in [122]), which turns out to be non degenerate, positive and will be denoted α in the following. All components of v are strictly positive and so $m_i = v_i / \sum_k v_k$. Notice that when a irreducible matrix M is also aperiodic then it is primitive (see Theorem 1.4 in [122]), that is there exists a positive integer k such that $(M^k)_{ij} > 0$ for all pairs of nodes i and j. This condition allows for a stronger version of the Perron-Frobenius theorem (compare Theorem 1.1 with Theorem 1.5).

5.4 ECOSYSTEM STABILITY

For this cooperative voter model we are able to relate key dynamical features of Eq. (59) to the topology of the interaction matrix M and prove analytically many results of ecological importance.

5.4.1 *Topology of the interaction network and stationary states*

Now, we discuss some features of the topology of the mutualistic interaction matrix M and how they relate to stationary states of the system.

A node with in-degree equals to zero and out-degree different from zero is called a *dead leaf* of the network. The operation of pruning consists in eliminating one by one the dead leaves of a given network together with their outbound links. After a first pruning, we will obtain a new network (that is a subnetwork of the starting one) that may still have dead leaves - the elimination of a dead leaf may create a new dead leaf. Going on with the pruning will result in a network that has no dead leaves. The latter network is called *pruned graph*. It is easy to see that the minimal pruned graph (i.e. with the smallest number of links) can be constructed on given S sites is the cyclic graph. More in general, we have:

Proposition: The stable network is a union of isolated nodes and graphs that contain at least one cycle each.

Indeed, pruning stops when the obtained graph is a union of isolated nodes and graphs where all nodes have at least an ancestor (i.e. the in-degree of each node is positive). Now a finite graph where each node has at least one incoming link contains at least a cycle. In fact, starting from one node it is possible to walk through the ancestors and never stop. Since the graph is finite, soon or later, the walker will visit twice the same node - so the walk contains a cycle - at most after a number of steps that equals the size of the graph.

Figure 11 shows an example of the pruning procedure and of a non-trivial pruned network.

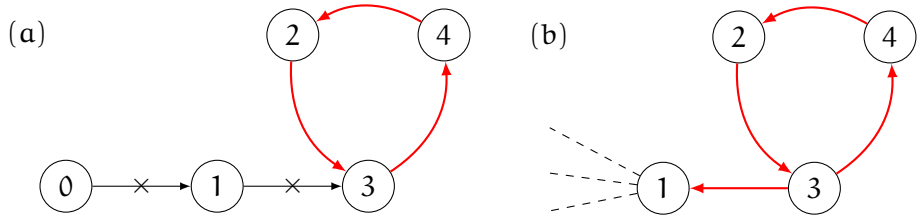

Figure 11: The diagram shows the pruning process. (a) An example of how the operation of pruning works. First the 0-node is eliminated with its outbound link. After that, the node 1 becomes a dead leaf and has to be pruned. The cycle shown by the red links is pruned graph with no dead leaves. (b) An example of pruned graph that is not made by cycles.

As we anticipated at the beginning of this section, the dynamics of species sitting on dead leaves of the interaction network is trivial as their relative abundance goes to zero. This is a simple consequence of the fact that a dead leaf has no incoming bond. Thus, when s is a dead leaf, the first term on the right of (59) is zero and simple estimate gives $\frac{d}{dt}\bar{\eta}^s \leqslant -\epsilon\,\bar{\eta}^s \sum_{i,j} \bar{\eta}^i M_{ij}\theta(\bar{\eta}^j)$. The previous simple remark leads to the following:

Limiting dynamics of dead leaves: Start the dynamics from a point with $\bar{\eta}^i \neq 0$ for all $i = 1,\dots,S$. If k is a dead leaf then $\lim_{t\to\infty} \bar{\eta}^k(t) = 0$.

In summary, the presence of a dead leaf inhibits species coexistence on the whole graph and coexistence is possible for the species that are nodes of the pruned sub-network. More precisely, if $i = 1,\dots,\gamma$ are dead leaves (at some step of the pruning), the stable equilibria must have $\bar{\eta}^1 = \dots = \bar{\eta}^\gamma = 0$. The extinction of the i-th may create new unsupported species that go to zero in the long run dynamics. Such a

cascade of extinctions eventually end only when all the nodes of the interaction network have non-zero in-degree.

5.4.2 *Stationary solution of the MF dynamics from the species interaction network*

If Perron-Frobenius theorem holds, then the initial condition is always not orthogonal to the right eigenvector, w, of M corresponding to the largest real eigenvalue α, and the time dependent solution of Eq. (59) is

$$\bar{\eta}(t) = \frac{\bar{\eta}(0)^T e^{Mt}}{\sum_i (\bar{\eta}(0)^T e^{Mt})_i} \tag{63}$$

Since for any eigenvalue, $\beta \neq \alpha$, of M we have $\Re(\beta) < \alpha$ the dominant term in both numerator and denominator in Eq. (63) is $v\, e^{\alpha t}(\bar{\eta}(0) \cdot w)$ leading to $\lim_{t\to\infty} \bar{\eta}(t) = \frac{v}{\sum_i v_i} = m$. This is an easy computation when M has a basis of eigenvectors and in general can be derived using the Jordan decomposition (appendix C).

As a corollary of the derivation above we have also that the stationary solution is globally stable. Therefore, within our framework, we can analytically study the impact of the species interaction network architecture on system stability and species extinction. In particular we found that both nested and modular structures observed in real ecological communities [123] satisfy the Perron-Frobenius theorem and contribute to the system stability. The results of the mean field predictions and the comparison with the corresponding stochastic dynamics are shown in Figure 12. Two simple examples are shown corresponding to an ecosystem with no extinction (panels A-C) and with extinction (panel D-F). When the mean field predicts the coexistence of all species then the stochastic dynamics leads to the first extinction over exponentially large time with the system size, N [124, 116].

5.4.3 *Stability of the equilibria*

As already shown in chapter 3, stability of the stationary states of the population dynamics is a key information of the ecological system. In particular is of great interest how the stability of the equlibria change for increasing ecosystem complexity [32, 47, 106, 23].

To study analytically the stability of the equilibria as a function of ecological complexity, we analyze the eigenvalues of the linearization of Eq. (59), i.e. the Jacobian matrix A, around the equilibria, m_i, of the system.

Following [47, 23] we assign the entry M_{ij} with probability C to be random a variable with positive mean μ, variance σ^2 and correlation ρ between non-zero off-diagonal elements M_{ij} and M_{ji}. The global

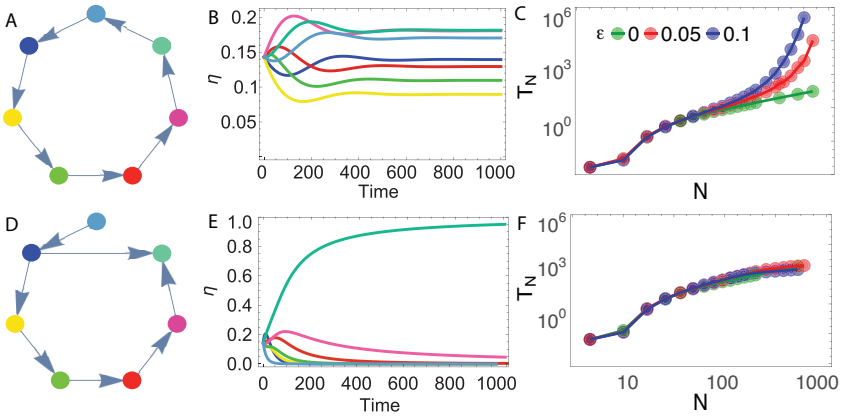

Figure 12: Upper panels: (A) Species interaction network for 7 species where each species has one mutualistic partner and all non-zero interaction $M_{ij} = 1$. (B) Time evolution of the populations of the 7 species as predicted by the mean field dynamics Eq. (59). (C) Average time for one of the 7 species to get extinct in the full stochastic dynamics. The average first extinction times grows exponentially with the system size, N, i.e. $T_N \sim exp(N)$. On the contrary if $\epsilon = 0$, the standard voter model, then $T_N \sim N$ [52]. Lower panels: (D) Species interaction network where one species is not helped by any species and the iterative pruning process, as described in the text, leads to no interaction network. (E) This causes a cascade of extinctions as the time evolution of the mean field Eq. (59) shows, leading to only one species dominating the community. (F) The corresponding average first extinction times of the microscopic stochastic model at various interaction strength, ϵ are all compatible with the $\epsilon = 0$ case.

mean, standard deviation and correlation coefficient are $\mu_M = C\mu$, $\sigma_M = \sqrt{C\left(\sigma^2 + (1-C)\mu^2\right)}$ and $\rho_M = \frac{\rho\sigma^2 + (1-C)\mu^2}{\sigma^2 + (1-C)\mu^2}$ [80].

If $\mu \geqslant \frac{\sigma(1+\rho)}{\sqrt{S}}$, the leading eigenvalue $\lambda_M \approx S\mu$ lies on the right of the ellipse formed by the others [23, 81]. The corresponding eigenvector has positive components according to Perron-Frobenius theorem [125] and its components are approximately constant, i.e. the equilibria of Eq. (59) can be written as

$$m_i = \frac{1}{S}(1 + \xi_i) \quad \text{for} \quad i = 1, \ldots, S \tag{64}$$

where $\sum_i \xi_i = 0$. Therefore $1 = Sm_i - \xi_i$

$$\begin{aligned}
\sum_{k=1}^{S} M_{ik} &= \sum_{k=1}^{S} M_{ik}\left(Sm_i - \xi_i\right) \\
&= S\sum_{k=1}^{S} M_{ik}m_i - \sum_{k=1}^{S} M_{ik}\xi_i \\
&\approx \sum_{ik}^{S} M_{ik}m_i - \sum_{k=1}^{S} M_{ik}\xi_i \\
&= \lambda_M - \sum_{k=1}^{S} M_{ik}\xi_i
\end{aligned}$$

The approximately equal holds when the degree of each node is similar as the average degree of all nodes.

$$\begin{aligned}
m_j \sum_{k=1}^{S} M_{ik} &= m_j(\lambda_M - \sum_{k=1}^{S} M_{ik}\xi_i) \\
&= m_j\lambda_M - m_j \sum_{k=1}^{S} M_{ik}\xi_i \\
&= \frac{1}{S}(1 + \xi_j)\lambda_M - \frac{1}{S}(1 + \xi_j) \sum_{k=1}^{S} M_{ik}\xi_i \\
&= \lambda_M/S + \xi_j\lambda_M/S - \sum_{k=1}^{S} M_{ik}\xi_i/S - \xi_j \sum_{k=1}^{S} M_{ik}\xi_i/S
\end{aligned}$$

All the terms involving ξ_i are sub-leading in S, so $m_j \sum_{k=1}^{S} M_{ik} \approx \lambda_M/S$.

Finally, we obtain

$$\begin{aligned}
J_{ij} &\approx M_{ij} - \lambda_M/S - \delta_{ij}\lambda_M \\
&= M_{ij} - \mu_M - \delta_{ij}S\mu_M \\
&= A_{ij} \ - \delta_{ij}S\mu_M
\end{aligned} \tag{65}$$

where $A_{ij} := M_{ij} - \mu_M$ is a random matrix with mean 0, standard deviation σ_M and correlation coefficient ρ_M. This implies that the

eigenvalues are uniformly distributed in an ellipse centered around $-S\mu_M$ with horizontal semi-axis $\sqrt{S}\sigma_M(1+\rho_M)$ and vertical semi-axis $\sqrt{S}\sigma_M(1-\rho_M)$ [23, 81]. The largest eigenvalue of the Jacobian matrix J_{ij} is given by $-S\mu+\sqrt{S}\sigma(1+\rho)$. If S is large enough ($S > \left(\frac{\sigma_M(1+\rho_M)}{\mu_M}\right)^2$), the system is always stable. Substituting the formulas of μ_M, σ_M and ρ_M to the center, horizontal semi-axis, vertical semi-axis and the largest eigenvalue discussed above, the final formulas are

$$\begin{aligned}
\text{ellipse center:} &\quad -CS\mu \\
\text{horizontal semiaxis:} &\quad \frac{C\sqrt{S}\left((\rho+1)\,\sigma^2-2(C-1)\mu^2\right)}{\sqrt{C\left(\sigma^2-(C-1)\mu^2\right)}} \\
\text{vertical semiaxis:} &\quad \frac{C\sqrt{S}\,(1-\rho)\,\sigma^2}{\sqrt{C\left(\sigma^2-(C-1)\mu^2\right)}} \\
\text{largest eigenvalue:} &\quad -CS\mu+\frac{C\sqrt{S}\left((\rho+1)\,\sigma^2-2(C-1)\mu^2\right)}{\sqrt{C\left(\sigma^2-(C-1)\mu^2\right)}}
\end{aligned} \tag{66}$$

If the connectivity C (or S) is fixed, as S (or C) increases, then the largest eigenvalue will decrease (Figure 13a and 13b). If the connectivity scale as $C \sim 1/S$, as S increases (or C decreases), the center of the ellipse will not change, the horizontal semi-axis will increase and the vertical semi-axis will decrease, then the largest eigenvalue will increase (Figure 13c and 13d). But if S is big enough, this change is ignorable comparing to the fixed center. Therefore, in the proposed model cooperation promotes ecosystem biodiversity, that in turn increases its stability without any fine tuning of the species interaction strengths nor of the self-interactions [80].

5.5 RELATIVE SPECIES ABUNDANCE

Finally we analyze the relative species abundance (RSA) of our simulated ecosystem. RSA is an important emergent pattern in ecology [82, 108, 84, 109, 107]. It describes commonness and rarity of species, thus characterizing the biodiversity of an ecological community. In the model, the RSA is exactly given by the mean field stationary solution $\mathbf{m}$, that in turn depends on the species interaction matrix M. The cumulative RSA is thus defined as the fraction of species with population greater that a certain value, n,

$$P_>[n] = \frac{1}{S}\sum_{k=1}^{S}\theta(n-Nm_k), \tag{67}$$

where we have fixed $N = 1/\min\{m_1,\dots,m_S\}$ when all species coexist, i.e. we have made the choice that the rarest species has population equal to 1. We numerically find that the shape of the stationary RSA weakly depends on the specific distribution of the matrix elements

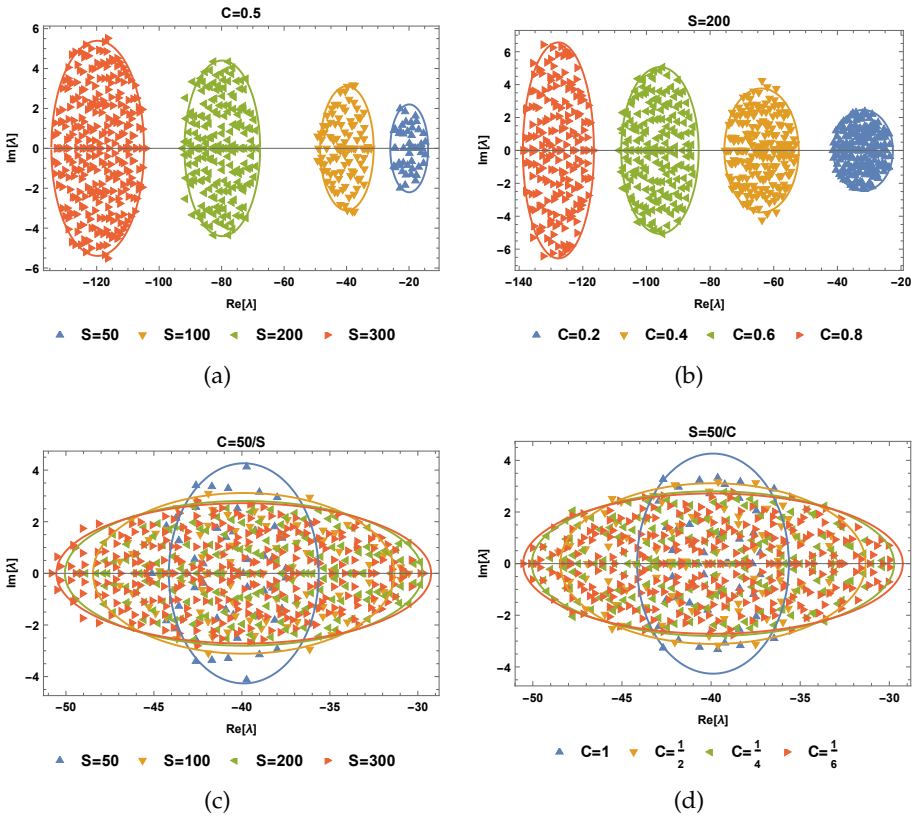

Figure 13: Stability for the relationship between size and connectivity. The matrix elements draw from the standard half-normal distribution. (a) The connectivity C is fixed; (b) The size S is fixed. (c) The connectivity depends on the size; (d) The size depends on the connectivity. The matrix M is generated by the standard half-standard normal distribution. The marker are the numeric eigenvalues of jacobian matrix J and the ellipse is its area analytically.

M_{ij}, and it is mainly determined only on its coefficient of variation $CV = \sigma_M/\mu_M$, i.e. the variability of the interaction strengths relative to the mean of M (see Figure 14). This allows to constrained the model parameters: In order to parametrize species interactions strengths, that are typically unknown [23, 7], we can make use of a random matrix approach where we fix the mean and the variance according to the desired RSA one needs to fit. Contrarily to what typically is done in the literature [126, 127, 78, 128] we also find that, for most of the structure of interaction matrix M, both the correlation matrix V and its inverse V^{-1} are not good proxies of the species interactions network - at least within our framework. This result highlights the importance to properly infer interaction networks from data [78] and this point is discussed in the next Chapter.

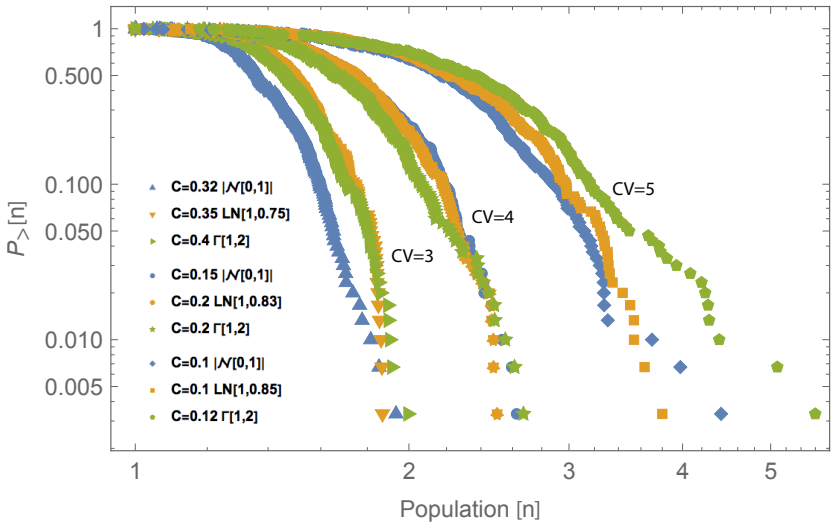

Figure 14: Cumulative RSA for 9 different species interaction random networks M, where matrix elements M_{ij} have been drawn from three different probability distributions: a Normal distribution $\mathcal{N}(\alpha, \beta)$ (blue lines) (M_{ij}'s are the the modulus of normally distributed random numbers), Gamma distribution $\Gamma(\alpha, \beta)$ (green lines) and LogNormal distribution $\mathrm{LN}(\alpha, \beta)$ (orange lines lines). We set the distribution parameters α, β (see legend) so that in each case we build interaction matrices with three different values of coefficient of variation $CV = \sigma_M/\mu_M = 3, 4, 5$. As we can see, the cumulative RSA is not very sensible to the distribution from which the matrix elements M_{ij} are drawn, but only on the CV. We highlight that in all the above cases $\rho = 0$, but we have non-zero correlation among elements of M as $\rho_M = \frac{\rho\sigma^2+(1-C)\mu^2}{\sigma^2+(1-C)\mu^2} \neq 0$. For example, in the first case, the distribution from which the elements are drawn is standard half-normal distribution $|\mathcal{N}(0, 1)|$, the connectivity $C = 0.32$, and the matrix correlation is $\rho_M = 0.543$.

5.6 Extension of our framework to meta-community population dynamics

Our framework can be generalized to model population dynamics in meta-communities, i.e. local ecological communities interacting among them [129, 130]. In this case, each node represent a community (see Figure 15), species interact within a community (and from each node of a community one can reach any other node of the same community following links (i, j) such that $M_{ij} > 0$), and communities interact among them.

5.6.1 *Ecological meta-community formed by two communites*

Considering the case of two communities A and B, connected by directional mutualism (known also as commensalism), where species

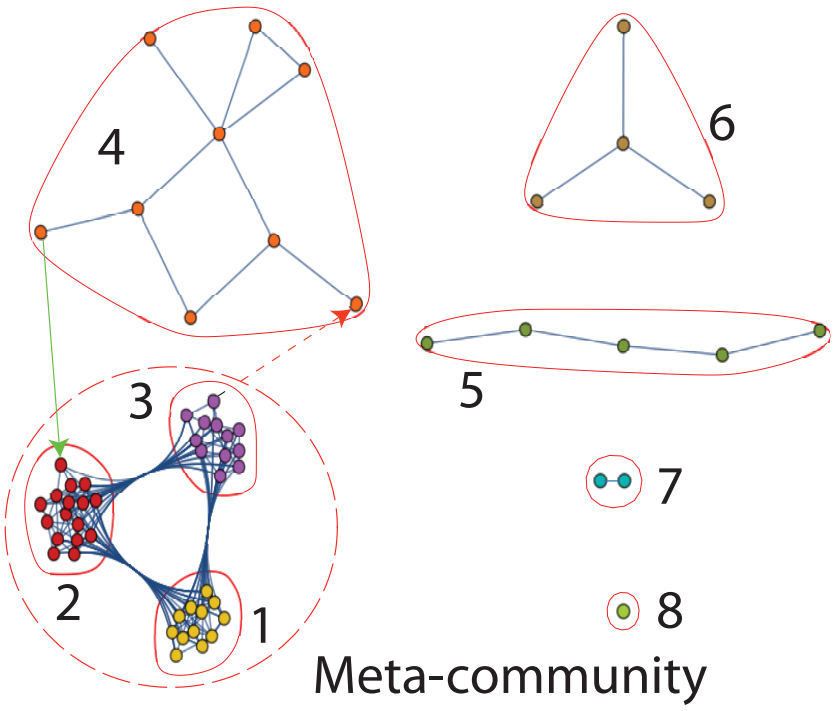

Figure 15: Meta-community framework. In this example the ecosystem is composed by 7 different communities. The three largest communities (1,2,3) interact among them and correspond to the giant strong connected component (red dashed line) of the global species interaction network M. The other communities composed fewer species are instead isolated. In this case, the Perron-Frobenius theorem does not hold, and in fact, if we ran the dynamics we observe extinctions. In particular, as predicted by our model, all isolated communities are going to be extinct (from community 7 to community 4) and only the species involved in the giant strongly connected cluster will survive. Adding a commensalism (green arrow) does not change the situation: only species in communities 1,2,3 will survive. However, if we add even a small reward for the community 4 by community 3, then the giant strongly connected cluster will be now composed by communities 1-4 and a larger number of species can coexist.

in community B benefit from the presence of some species in community A (e.g. sea turtles in community A and pilot fish (Naucrates ductor) in fish community B), the species interaction in this ecosystem are described by a matrix of the form $M = \begin{pmatrix} A & X \\ 0 & B \end{pmatrix}$ where A (B) is a $S_A \times S_A$ ($S_B \times S_B$) matrix, $M_{ij} \geqslant 0 \, \forall i, j = 1, ..S$, $S = S_A + S_B$ and the corresponding species abundances are $m_A \in \mathbb{R}_+^{S_A}$, $m_B \in \mathbb{R}_+^{S_B}$ where $(m_A, m_B) = m$ and $\sum_{i=1}^{S} m_i = 1$ (Fig. 16 (a) is a simple diagram). The analytic solution of the mean-field equation is $(m_A, m_B) M = \alpha (m_A, m_B)$. Because $m_A A = \alpha m_A$ is independent of B, we could

apply previous method based on Perron-Frobenius theorem [125] to obtain the m_A ($\alpha > 0$ and $m_A > 0$). Then $m_A X + m_B B = \alpha m_B$, therefore $m_B = m_A X (\alpha I_{S_B} - B)^{-1}$. Let β be the eigenvalue of B (for Perron-Frobenius theorem $\beta > 0$) with the largest modulus. If $\beta < \alpha$, $(\alpha I_{S_B} - B)^{-1} = \frac{1}{\alpha} \sum_{k=0}^{\infty} \left(\frac{B}{\alpha}\right)^k > 0$ since B is primitive. Because $X \geqslant 0$, $m_B > 0$. This result can be generalized to three or more communities, A, B, ..., Z connected by directional mutualism.

5.6.2 *Ecological meta-community formed by three communites*

We generalize the same approach to three communities $M = \begin{pmatrix} A & X_1 & Y \\ 0 & B & X_2 \\ 0 & 0 & C \end{pmatrix}$ where $S = S_A + S_B + S_C$ (Fig. 16 (b) is a simple diagram) and the corresponding species abundances are $m_A \in \mathbb{R}_+^{S_A}$, $m_B \in \mathbb{R}_+^{S_B}$, $m_C \in \mathbb{R}_+^{S_C}$ where $(m_A, m_B, m_C) = m$ and $\sum_{i=1}^{S} m_i = 1$, the new mean-field equation is $(m_A, m_B, m_C) M = \alpha (m_A, m_B, m_C)$. Because $m_A A = \alpha m_A$ is independent of B and C, we could apply previous method based on Perron-Frobenius theorem to obtain the m_A ($\alpha > 0$ and $m_A > 0$). According to the above case, $m_B = m_A X_1 (\alpha I_{S_B} - B)^{-1} > 0$ if $\beta < \alpha$. Similarly, $m_C = (m_A Y + m_B X_2)(\alpha - C)^{-1} > 0$ if $\gamma < \alpha$

Notice that $X_1 = 0$ (i.e. C is helped both by A and B, but A and B are independent) implies that $m_B = 0$. A and B in this case are intangible, so there are two stationary states. One is A extinct, the other is B extinct!

5.6.3 *Generalization to Ecological meta-community formed by any number of communites*

In general, if $M = \begin{pmatrix} A & X_{AB} & \cdots & X_{AZ} \\ 0 & B & \cdots & X_{BZ} \\ 0 & 0 & \ddots & \vdots \\ 0 & 0 & \cdots & Z \end{pmatrix}$ (Fig. 16 (c) is a simple diagram) and the Perron-Frobenius eigenvalue of A, λ_A is larger than Perron-Frobenius eigenvalues of other communities $(\lambda_B, \lambda_C, \cdots)$, there is no extinction in this ecology system.

Beside conditions for meta-communities coexistence, this generalization allows us to understand which species or communities will go extinct based on the topological properties of the species interaction networks. In particular, if $X_{IZ} \geqslant 0$ and $X_{ZI} = 0$ for all $I = A, B, ..., Y$ and all other $X_{K,L} = 0$ for $K \neq L$, then the community Z is helped by all other communities that in turn are independent to one another. In this case all communities except Z is going to be extinct. More generally, as shown in Figure 15, isolated species or communities are

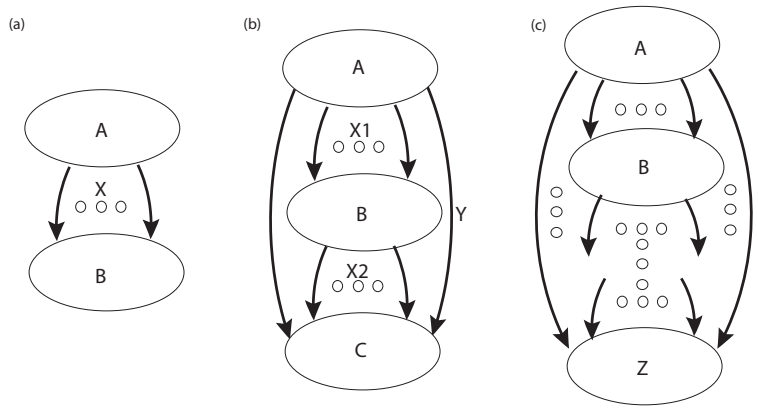

Figure 16: Mutualistic meta-community diagram. (a) two meta-communities; (b) three meta-communities; (c) many meta-communities.

going to be extinct if they do not belong to the largest cluster. This result suggests that reciprocated cooperation play an important role in selecting the coexisting species: species/communities that cooperate (or cooperate more) have competitive advantages with respect to other species/communities that do not cooperate (or cooperate less) and that are thus doomed to extinction.

6

SPECIES COVARIANCE AND INTERACTION MATRIX

Real knowledge is to know the extent of one's ignorance.

— Confucius (551 BC - 479 BC)

6.1 INTRODUCTION

Recognizing relationships between variables connected in a network is a pervasive problem in biology [131, 132, 133], ecology [78, 134, 128] and information sciences [135, 136, 137], just to cite few. How strong are the interactions among species, which type are them and what impact do they have on the whole ecosystem is perhaps the most fundamental problem in community ecology for understanding patterns of coexistence and the distribution and abundance of species. As already see in Chapter 3, the interactions between two species in a ecosystem may be of different types: Mutualism (++), Parasitism/Predation (+-), Amensalism (-o), Commensalism (+o) and Competition (+-) (see Fig. 6 for details).

Unfortunately, detecting these various types of interactions and reconstructing the whole ecological network is far from straightforward and existing approaches are limited. Novel approaches can also open the way towards global models of ecosystem dynamics and such models will ultimately be able to predict the outcome of community alterations and the effects of perturbations.

6.1.1 *Covariance or correlation matrix*

One general method is applying the covariance/correlation of the population of two observed species as the interdependency to construct the whole interaction network. The covariance/correlation matrix is a matrix whose element in the i, j position is the covariance/-correlation coefficient between the i-th and j-th entry of the vector describing the species population abundance. It can be written as

$$\mathrm{cor}(X) = (\mathrm{diag}(\Sigma))^{-\frac{1}{2}}\,\Sigma\,(\mathrm{diag}(\Sigma))^{-\frac{1}{2}} \tag{68}$$

where $\Sigma = E\left[(X - E[X])(X - E[X])^T\right]$, $\mathrm{diag}(\Sigma)$ is the diagonal matrix of Σ. Although it is easy to calculate and understand, it contains numerous indirect relationships and correlation does not provide the direct insight on if and how two species interact.

6.1.2 *Interaction matrix inferred through the maximum entropy principle*

The principle of maximum entropy [138, 139] provides another simple method to infer the probability distribution in an unbiased manner using the measured average populations and correlation functions as an input [134, 140, 127]. Its aim is to find the probability distribution function $p(\vec{x})$ that maximizes the Shannon entropy

$$S = -\sum_{\vec{x}} p(\vec{x}) \ln(p(\vec{x})) \tag{69}$$

subject to the constraint that

$$\sum_{\vec{x}} p(\vec{x}) = 1 \tag{70}$$

$$\langle x_i \rangle = \sum_{\vec{x}} p(\vec{x}) x_i = \frac{1}{T} \sum_{T} x_i^k \tag{71}$$

$$\langle x_i, x_j \rangle = \sum_{\vec{x}} p(\vec{x}) x_i x_j = \frac{1}{T} \sum_{T} x_i^k x_j^k \tag{72}$$

where $\vec{x} = (x_1, ..., x_N)$ is the state vector for N species and T is the length of observed data.

Eq. (70) provides the normalization condition that the probabilities of all observable states sum to 1 as well as Eqs. (71) and (72) ensure that the distribution $p(\vec{x})$ preserves the mean and the correlations observed in the dataset, so the matrix element M_{ij} has the natural interpretation of the interaction between the i-th and j-th species. Its Boltzmann-like distribution $p(x) \sim e^{-H}$ where $H = 1/2 \sum_{ij} x_i V_{ij} x_j$ plays the role of the energy function in conventional statistical mechanics. The interaction matrix can be obtained by inverting the matrix of covariance matrix, $V_{ij}^{-1} = C_{ij} = \langle x_i, x_j \rangle - \langle x_i \rangle \langle x_j \rangle$. It provides a measure of the effective interactions while faithfully encoding all available information (if mean and correlations are the only available information) and being unbiased with respect to missing information.

In this section, we consider the normal fluctuations around the deterministic limit of Eq. (59). This allows us to calculate the pair-wise covariance matrix V between pairs of species population abundances [134]. This quantity, once opportunely thresholded, is used as an empirical proxy of the species interactions network [78, 141, 126]. Other works, applying maximum entropy approach, use V^{-1} as the quantity to describe species interactions [134, 127]. The aim of this section is to test how well V or V^{-1} approximate the true interactions described by M in our model.

In our setting, we can compute analytically the covariance matrix in the limit of normal fluctuations. We define species abundance fluctuations as $x_N^i(t) = \sqrt{N}\left(\bar{\eta}^i(t) - m_i\right)$ for $i = 1, \dots, S$. Again, one can apply standard techniques of convergence of generators to get weak convergence to the thermodynamic limiting evolution [121]. Indeed, the stochastic process $\left(x_N^1(t), \dots, x_N^S(t)\right)$ converges in distribution to a Gaussian Markov process $X := \left(X^1(t), \dots, X^S(t)\right)$ which solves the stochastic differential equation

$$dX = \epsilon\, A X\, dt + \Phi\, dB_t, \tag{73}$$

where B_t is a S-dimensional Brownian motion, which corresponds to a S-dimensional Ornstein-Uhlenbeck process [121, 83]. The matrices A and Φ depend on the interaction matrix M and the equilibria of Eq. (59), i.e.

$$A_{ij} = M_{ji} - \delta_{ij} \sum_{h,k=1}^{S} m_h M_{hk} - m_i \sum_{k=1}^{S} M_{jk}, \tag{74}$$

and Φ satisfies the following constraint equation

$$\begin{aligned} (\Phi\Phi^T)_{ij} = &-2\left(m_i m_j + \epsilon m_i \sum_{k=1}^{S} m_k M_{kj}\right)(1-\delta_{ij}) \\ &+ 2(1-m_i)\left(m_i + \epsilon \sum_{k=1}^{S} m_k M_{ki}\right)\delta_{ij} \end{aligned} \tag{75}$$

where δ_{ij} is the Kronecker delta.

From Eq. (73), it is then possible to derive the dynamics of the covariance matrix $V_{ij}(t) = \langle X^i(t), X^j(t)\rangle$ (see [114] for details). Therefore, we have

$$\frac{dV}{dt} = \epsilon\, A\, V(t) + \epsilon\, V(t)\, A^T + \Phi\Phi^T, \tag{76}$$

and at the equilibrium the covariance matrix resolves the following equation

$$\epsilon\, A\, V^{eq} + \epsilon\, V^{eq}\, A^T + \Phi\Phi^T = 0. \tag{77}$$

Eq. (77) is a Lyapunov equation, so we could apply standard algorithms to solve it numerically [142].

6.2.1 *empty sites*

Analogous of formula (76) and (77) holds true for for the model with empty sites, but for different A and Φ. In fact in this case, the linearized dynamics described by the matrix $\tilde{A}_{ij}$ with $0 \leqslant i, j \leqslant S$ reads:

$$
\begin{aligned}
\tilde{A}_{00} &= -2\,\epsilon \sum_{i,k=1}^{S} M_{ki} m_k \\
\tilde{A}_{0j} &= -\epsilon\, m_0 \sum_{k=1}^{S} M_{jk} && \text{for } j = 1,\dots,S \\
\tilde{A}_{i0} &= m_i + \epsilon \sum_{k=1}^{S} M_{ki} m_k && \text{for } i = 1,\dots,S \\
\tilde{A}_{ij} &= (m_0 - \lambda)\delta_{ij} + \epsilon\, m_0 M^{T}_{ij} + \epsilon A_{ij} && \text{for } i,j = 1,\dots,S
\end{aligned}
$$

while the diffusion matrix $\tilde{\Phi}_{ij}$ with $0 \leqslant i,j \leqslant S$ is

$$
\begin{aligned}
(\tilde{\Phi}\tilde{\Phi}^{T})_{00} &= (1-m_0)(1+\lambda) + \epsilon \sum_{k,h=1}^{S} M_{kh} m_k \\
(\tilde{\Phi}\tilde{\Phi}^{T})_{0j} &= -2m_j\,\lambda && \text{for } j = 1,\dots,S \\
(\tilde{\Phi}\tilde{\Phi}^{T})_{i0} &= -2m_i + 2\epsilon \sum_{k=1}^{S} M_{ki} m_k && \text{for } i = 1,\dots,S \\
(\tilde{\Phi}\tilde{\Phi}^{T})_{ij} &= (\Phi\Phi^{T})_{ij} && \text{for } i,j = 1,\dots,S \\
(\tilde{\Phi}\tilde{\Phi}^{T})_{ii} &= m_i\,\lambda + m_i + \epsilon \sum_{k=1}^{S} M_{ki} m_k + (\Phi\Phi^{T})_{ii} && \text{for } i = 1,\dots,S
\end{aligned}
$$

6.3 SPECIES INTERACTION MATRIX

By inverting the solution of Eq. (77), we calculate the inverse of the covariance matrix. In fact, V^{-1} in a Gaussian model or in a Gaussian approximation corresponds to the species interaction matrix [140, 134]. Indeed, within a maximum Entropy approach, V^{-1} is typically used to infer species interactions based on the available information of the system [127]. In our framework and as shown by Eq.(76), the relation between the interaction matrix M and the matrix V or V^{-1} is highly non-linear. Moreover, because of the constraint on the matrix V, $\sum_j V_{ij} = 0$, then V is not invertible, and thus in order to compute V^{-1} we apply a pseudo-inverse scheme. Results are shown for the model without empty sites, but there is no qualitatively difference with empty sites. As shown in Figures 17-18, even for very simple structure of matrix M, V and V^{-1} are not good proxies of the species interactions. Although using our model shows that no of these methods work, this result highlights the importance to properly infer interaction networks from data. Therefore, how to explain the interaction of each species is still an open problem.

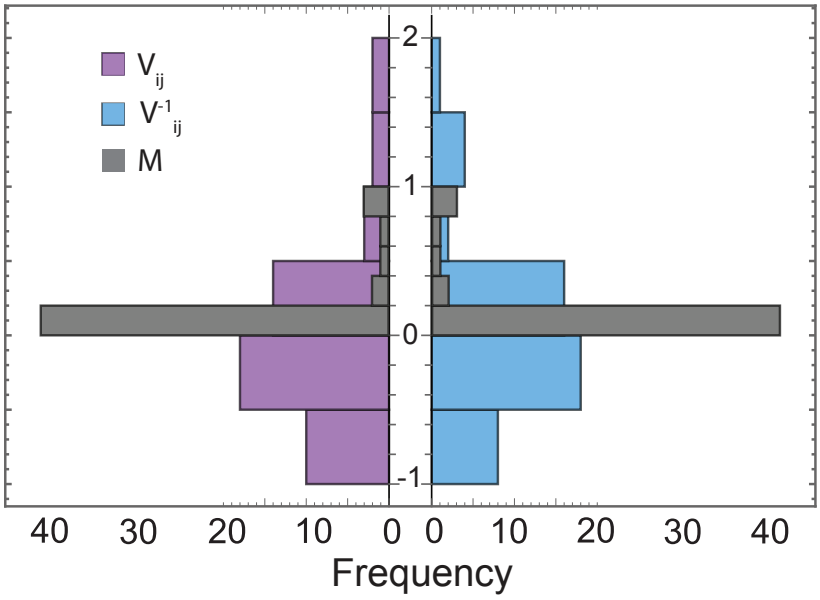

Figure 17: Histogram with the elements of the covariance Matrix V and its inverse V^{-1} (calculated using pseudo-inverse method) compared to the actual species interaction network M for a small (S=7) and sparse (C=1/(S-1)) species interaction network. We see that both V and V^{-1}, if used as a proxy of M, overestimate the real interactions in the ecological community.

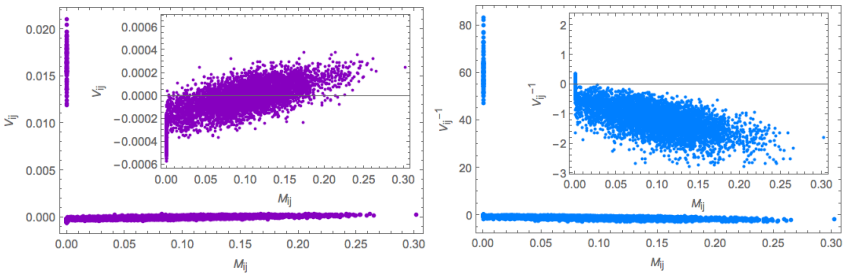

Figure 18: Elements of the covariance matrix V and its inverse V^{-1} (calculated using pseudo-inverse method) compared to the actual species interaction network M for a large (S=100) and dense (C=0.5) network. We see that, although there is some significant correlations between elements of V, V^{-1} and M (see inset) , many actual interactions ($M_{ij} \neq 0$) are set to zero in both V and V^{-1}. On the other hand, in both V and V^{-1} wrongly indicate species interactions also if $M_{ij} = 0$.

Part III

APPENDIX

A

MEAN-FIELD APPROXIMATION

As given by Eq. (5), the activity of each node depends on itself ($F(x_i)$) and on the interaction with its nearest neighbours ($\sum_{j=1}^{S} A_{ij} G(x_i, x_j)$). Therefore, the activity of the average nearest neighbours nodes represent an important contribution of the system dynamics.

Assuming y_i is a scalar quantity related to node i, we can define the mean value of y over all nodes as y_i is $\langle y_i \rangle = \frac{\sum_{i=1}^{S} y_i}{S}$. For a given node i, and picking at random another node j, the probability that the selected j is a neighbour of node i is proportional to the out-degree of j, $s_j^{out} = \sum_{i=1}^{S} A_{ij}$. Therefore, the larger the out-degree of node j is, the larger will be the probability to select node j. We can thus define the mean over all nearest neighbour nodes as

$$\langle y_j \rangle_{nn} = \frac{\frac{1}{S}\sum_{j=1}^{S} s_j^{out} y_j}{\frac{1}{S}\sum_{j=1}^{S} s_j^{out}}. \tag{78}$$

Defining $y_j(x_i) = G(x_i, x_j)$, the second term of the right part of Eq. (5) could be written as: $\sum_{j=1}^{S} A_{ij} G(x_i, x_j) = s_i^{in} \langle y_j(x_i) \rangle_{j(i)}$, where $j(i)$ denote all the neighbour nodes of i and $s_i^{in} = \sum_j^S A_{ij}$ is the in-degree of node i. We highlight that if the correlations among the nodes degree of the network given by the adjacency matrix A are small, then the neighbour of i is on average representative of the neighbour of any other other nodes and the relation $s_i^{in} \langle y_j(x_i) \rangle_{j(i)} = s_i^{in} \langle y_j(x_i) \rangle_{nn}$ holds for each pair of nodes i and j.

In order to mathematically formalize the above analysis, the operator $\mathcal{L}(y) = \frac{\mathbf{1}^T \mathbf{A} y}{\mathbf{1}^T \mathbf{A} \mathbf{1}} = \frac{\frac{1}{S}\sum_{j=1}^{S} s_j^{out} y_j}{\frac{1}{S}\sum_{j=1}^{S} s_j^{out}}$ is introduced, where $\mathbf{1} = (1, ..., 1)^T$ is the unit vector. According to this operator, Eq. (5) can be written as $\frac{dx_i}{dt} = F(x_i) + s_i^{in} \mathcal{L}\left(G(x_i, \mathbf{x})\right)$. If $G(x_i, x_j)$ is linear in x_j or the variance in the components of $\mathbf{x}$ is small, then $\mathcal{L}\left(G(x_i, \mathbf{x})\right) \approx G(x_i, \mathcal{L}(\mathbf{x}))$. Therefore, $\frac{dx_i}{dt} \approx F(x_i) + s_i^{in} G\left(x_i, \mathcal{L}(\mathbf{x})\right)$ and the vector notation is $\frac{d\mathbf{x}}{dt} \approx F(\mathbf{x}) + \mathbf{s}^{in} \circ G\left(\mathbf{x}, \mathcal{L}(\mathbf{x})\right)$, where $\circ$ is the Hadamard product. By applying the operator to both sides of vectorized equation, it changes to:

$$\frac{d\mathcal{L}(\mathbf{x})}{dt} \approx \mathcal{L}\left(F(\mathbf{x}) + \mathbf{s}^{in} \circ G(\mathbf{x}, \mathcal{L}(\mathbf{x}))\right) \approx F\left(\mathcal{L}(\mathbf{x})\right) + \mathcal{L}(\mathbf{s}^{in}) G\left(\mathcal{L}(\mathbf{x}), \mathcal{L}(\mathbf{x})\right). \tag{79}$$

Eq. (79) gives us the mean field description of the network activity, but where the mean-field has been carried on in two steps: first averaging only over the neighbours nodes, and then averaging again over the whole network. Thanks to this mean-field approach we have a

one-dimensional description of the complex multi-dimensional equation give by Eq. (5).

B

ALGORITHM TO CALCULATE THE MEAN OF COMBINATION

The algorithm to calculate the mean of combination of d and n consists of the following steps:

1. **Generation of a feasible index combination.** Such a combination like $(i = j \neq k \neq l, i \neq l)$ is encoded in the upper triangle of a 4×4 boolean matrix, which in this case would look like

$$P = \begin{bmatrix} - & T & F & F \\ - & - & F & F \\ - & - & - & F \\ - & - & - & - \end{bmatrix} . \tag{80}$$

   Here, $P_{ij} = T$ implies that the i-th index is equal to the j-th index (F for $\neq$), numbering the indices as $(i, j, k, l) \sim (0, 1, 2, 3)$. We dump non-feasible combinations such as

$$P_{\text{illegal}} = \begin{bmatrix} - & T & F & F \\ - & - & F & T \\ - & - & - & F \\ - & - & - & - \end{bmatrix} . \tag{81}$$

2. **Calculating the number of terms n_P associated with P.** In order to do so, we sort the indices into cliques containing only equal ones. The number of cliques, called multiplicity factor m_P is directly related to the number of terms by

$$n_P = S(S-1)...(S-m_P) = \prod_{\alpha=0}^{m_P-1} (S-\alpha) . \tag{82}$$

3. **Project the matrix P down to a 2×2 boolean matrix R_P.** This matrix encodes whether the actual random variables $X = A_{ij}$ and $Y = A_{kl}$ are equal. We have $X = Y$ only if $i = k$ and $j = l$, which in terms of the matrices P and R_P is stated as

$$R_{01}(P) = P_{02} \wedge P_{13} . \tag{83}$$

4. **Calculating actual cliques** $\mathcal{C}(R(P))$**.** In this case, the only possible cliques are XY or X^2, trivially encoded by $R_{01}(P)$.

5. **Add contribution to overall sum.** Each clique is associated with a specific factor arising from taking the expected value. In this case, we only have

$$\langle XY \rangle = \mu^2 \qquad \text{and} \qquad \left\langle X^2 \right\rangle = \sigma^2 + \mu^2 \,. \tag{84}$$

We sum each term multiplied by the multiplicity n_P, iterating over all feasible index matrices P to get the corresponding expected value

$$\langle d \rangle = S \cdot \sum_P n_P \, \langle \mathcal{C}(R(P)) \rangle \,. \tag{85}$$

To incorporate correlation of transposed entries, we make use of the lower triangle of R. In this example, we have $A_{ij} = X$ and $A_{kl} = A_{ji} = X^T$ only if $i = l$, $j = k$ and $(i, j) \neq (k, l)$, that is

$$R_{10}(P) = P_{03} \wedge P_{12} \wedge \neg R_{01}(P) \,. \tag{86}$$

The associated clique has the expected value

$$\left\langle XX^T \right\rangle = \rho\sigma^2 + \mu^2 \,. \tag{87}$$

If we finally want to allow for the diagonal elements to be drawn from a different distribution, we employ the free diagonal in a similar manner. In this example:

$$R_{00}(P) = P_{01}, \qquad R_{11}(P) = P_{23} \,, \tag{88}$$

and the associated expected values

$$\langle XY_d \rangle = \mu\mu_d, \qquad \langle X_d Y_d \rangle = \mu_d^2, \qquad \left\langle X_d^2 \right\rangle = \sigma_d^2 + \mu_d^2 \,. \tag{89}$$

For the second order terms, R becomes a 4×4 boolean matrix, and the full set of possible cliques becomes both larger (30 terms for both correlation and specific diagonal) and more complicated (incorporating higher moments such as $\left\langle X^3 Y \right\rangle$).

C

JORDAN DECOMPOSITION

Jordan normal form is a basic tool in linear algebra. Here, for sake of completeness, we state the Jordan Normal Form theorem for a S-dimensional matrix M with entries $M_{ij} \in \mathbb{C}$. Before stating the theorem let us recall that a Jordan block of order k has the form

$$J = \begin{pmatrix} a_k & \xi_1 & 0 & \cdots & 0 & \\ 0 & a_k & \xi_2 & 0 & \cdots & 0 \\ \cdots & \cdots & \cdots & \cdots & \cdots & \\ 0 & \cdots & \cdots & 0 & a_k & \xi_s \\ 0 & \cdots & \cdots & \cdots & 0 & a_k \end{pmatrix} \tag{90}$$

where $a_k \in \mathbb{C}$ and $\xi_i \in \{0, 1\}$ for $i = 1, \ldots, k$.

The Jordan Normal Form theorem states that every endomorphism on a finite dimensional vector space on $\mathbb{C}$ has a Jordan matrix representation.

Jordan Normal Form: Let V be a finite dimensional vector space on $\mathbb{C}$ and M an endomorphism on V. Then there exits a basis of V such that, with respect to this basis, the endomorphism M has the representation

$$M = \begin{pmatrix} J_1 & 0 & 0 & \cdots & 0 \\ 0 & J_2 & 0 & \cdots & 0 \\ \cdots & \cdots & \cdots & \cdots & \cdots \\ 0 & \cdots & 0 & J_{m-1} & 0 \\ 0 & \cdots & 0 & 0 & J_m \end{pmatrix} \tag{91}$$

where J_i, $i = 1, \ldots, m$ are Jordan blocks. The number and the order of the blocks are unequivocally determined by M.

Then, for example, if the $i-$th block, J_i, has dimension d, and $v_1^i, v_2^i, \ldots, v_d^i$ are the vectors of the basis of the Jordan representation related to the $i-$th block, the Jordan Normal Form theorem implies that $M v_1^i = a_i v_1^i$ and $M v_j^i = a_i v_j^i + \xi_j v_{j-1}^i$ for $j = 2, \ldots, d$.

BIBLIOGRAPHY

[1] Erik Hollnagel, David D Woods, and Nancy Leveson. *Resilience engineering: concepts and precepts*. Ashgate Publishing, Ltd., 2007.

[2] Samir Suweis, Joel A Carr, Amos Maritan, Andrea Rinaldo, and Paolo D'Odorico. Resilience and reactivity of global food security. *Proceedings of the National Academy of Sciences*, 112(22):6902–6907, 2015.

[3] Donald R Nelson, W Neil Adger, and Katrina Brown. Adaptation to environmental change: contributions of a resilience framework. *Annual review of Environment and Resources*, 32(1):395, 2007.

[4] Carl Folke. Resilience: The emergence of a perspective for social–ecological systems analyses. *Global environmental change*, 16(3):253–267, 2006.

[5] Brian Walker, Crawford S Holling, Stephen R Carpenter, and Ann Kinzig. Resilience, adaptability and transformability in social–ecological systems. *Ecology and society*, 9(2):5, 2004.

[6] Samir Suweis and Paolo D'Odorico. Early warning signs in social-ecological networks. *PloS one*, 9(7):e101851, 2014.

[7] Samir Suweis, Filippo Simini, Jayanth R Banavar, and Amos Maritan. Emergence of structural and dynamical properties of ecological mutualistic networks. *Nature*, 500(7463):449–452, 2013.

[8] Martin A Nowak, Akira Sasaki, Christine Taylor, and Drew Fudenberg. Emergence of cooperation and evolutionary stability in finite populations. *Nature*, 428(6983):646, 2004.

[9] Albert-László Barabási and Réka Albert. Emergence of scaling in random networks. *science*, 286(5439):509–512, 1999.

[10] John H Holland. *Emergence: From chaos to order*. OUP Oxford, 2000.

[11] Jianxi Gao, Baruch Barzel, and Albert-László Barabási. Universal resilience patterns in complex networks. *Nature*, 530(7590):307–312, 2016.

[12] Marten Scheffer, Jordi Bascompte, William A Brock, Victor Brovkin, Stephen R Carpenter, Vasilis Dakos, Hermann Held,

Egbert H Van Nes, Max Rietkerk, and George Sugihara. Early-warning signals for critical transitions. *Nature*, 461(7260):53–59, 2009.

[13] Marten Scheffer, Stephen R Carpenter, Timothy M Lenton, Jordi Bascompte, William Brock, Vasilis Dakos, Johan Van De Koppel, Ingrid A Van De Leemput, Simon A Levin, Egbert H Van Nes, et al. Anticipating critical transitions. *science*, 338(6105):344–348, 2012.

[14] Marten Scheffer. *Critical transitions in nature and society*. Princeton University Press, 2009.

[15] Anthony R Ives. Measuring resilience in stochastic systems. *Ecological Monographs*, 65(2):217–233, 1995.

[16] SR Carpenter and WA Brock. Rising variance: a leading indicator of ecological transition. *Ecology letters*, 9(3):311–318, 2006.

[17] Chengyi Tu, Yuhua Cheng, and Kai Chen. Estimating the varying topology of discrete-time dynamical networks with noise. *Central European Journal of Physics*, 11(8):1045–1055, 2013.

[18] YY Liu, JJ Slotine, and AL Barabási. Controllability of complex networks. *Nature*, 473(7346):167–173, 2011.

[19] William Bialek. *Biophysics: searching for principles*. Princeton University Press, 2012.

[20] Baruch Barzel and Albert-László Barabási. Universality in network dynamics. *Nature physics*, 9:673, 2013.

[21] Sui Huang, Gabriel Eichler, Yaneer Bar-Yam, and Donald E Ingber. Cell fates as high-dimensional attractor states of a complex gene regulatory network. *Physical review letters*, 94(12):128701, 2005.

[22] Guy Karlebach and Ron Shamir. Modelling and analysis of gene regulatory networks. *Nature Reviews Molecular Cell Biology*, 9(10):770–780, 2008.

[23] Stefano Allesina and Si Tang. Stability criteria for complex ecosystems. *Nature*, 483(7388):205–208, 2012.

[24] Samir Suweis, Jacopo Grilli, Jayanth R Banavar, Stefano Allesina, and Amos Maritan. Effect of localization on the stability of mutualistic ecological networks. *Nature communications*, 6, 2015.

[25] Jacopo Grilli, Matteo Adorisio, Samir Suweis, György Barabás, Jayanth R Banavar, Stefano Allesina, and Amos Maritan. Feasibility and coexistence of large ecological communities. *Nature Communication*, 8, 2017.

[26] C Ronnie Drever, Garry Peterson, Christian Messier, Yves Bergeron, and Mike Flannigan. Can forest management based on natural disturbances maintain ecological resilience? *Canadian Journal of Forest Research*, 36(9):2285–2299, 2006.

[27] Jos Barlow, Gareth D Lennox, Joice Ferreira, Erika Berenguer, Alexander C Lees, Ralph Mac Nally, James R Thomson, Silvio Frosini de Barros Ferraz, Julio Louzada, Victor Hugo Fonseca Oliveira, et al. Anthropogenic disturbance in tropical forests can double biodiversity loss from deforestation. *Nature*, 535(7610):144–147, 2016.

[28] Stephan Barthel and Christian Isendahl. Urban gardens, agriculture, and water management: Sources of resilience for long-term food security in cities. *Ecological Economics*, 86:224–234, 2013.

[29] Yossi Sheffi et al. The resilient enterprise: overcoming vulnerability for competitive advantage. *MIT Press Books*, 1, 2005.

[30] Crawford S Holling. Resilience and stability of ecological systems. *Annual review of ecology and systematics*, pages 1–23, 1973.

[31] Ricard V Sole and M^{a} Montoya. Complexity and fragility in ecological networks. *Proceedings of the Royal Society of London B: Biological Sciences*, 268(1480):2039–2045, 2001.

[32] Robert McCredie May. *Stability and complexity in model ecosystems*, volume 6. Princeton university press, 2001.

[33] Boris Worm, Edward B Barbier, Nicola Beaumont, J Emmett Duffy, Carl Folke, Benjamin S Halpern, Jeremy BC Jackson, Heike K Lotze, Fiorenza Micheli, Stephen R Palumbi, et al. Impacts of biodiversity loss on ocean ecosystem services. *science*, 314(5800):787–790, 2006.

[34] Carl Folke, Steve Carpenter, Brian Walker, Marten Scheffer, Thomas Elmqvist, Lance Gunderson, and Crawford Stanley Holling. Regime shifts, resilience, and biodiversity in ecosystem management. *Annual Review of Ecology, Evolution, and Systematics*, 35, 2004.

[35] José M Montoya, Stuart L Pimm, and Ricard V Solé. Ecological networks and their fragility. *Nature*, 442(7100):259, 2006.

[36] Charles Boone, Howard Bussey, and Brenda J Andrews. Exploring genetic interactions and networks with yeast. *Nature reviews. Genetics*, 8(6):437, 2007.

[37] Andrew Pomerance, Edward Ott, Michelle Girvan, and Wolfgang Losert. The effect of network topology on the stability

of discrete state models of genetic control. *Proceedings of the National Academy of Sciences*, 106(20):8209–8214, 2009.

[38] Eitan Gross. Statistical mechanics of scale-free gene expression networks. *EPL (Europhysics Letters)*, 100(5):58004, 2012.

[39] Hae-Jeong Park and Karl Friston. Structural and functional brain networks: from connections to cognition. *Science*, 342(6158):1238411, 2013.

[40] Sophie Achard, Raymond Salvador, Brandon Whitcher, John Suckling, and ED Bullmore. A resilient, low-frequency, small-world human brain functional network with highly connected association cortical hubs. *Journal of Neuroscience*, 26(1):63–72, 2006.

[41] Danielle Smith Bassett and ED Bullmore. Small-world brain networks. *The neuroscientist*, 12(6):512–523, 2006.

[42] David Lusseau. The emergent properties of a dolphin social network. *Proceedings of the Royal Society of London B: Biological Sciences*, 270(Suppl 2):S186–S188, 2003.

[43] W Neil Adger, Terry P Hughes, Carl Folke, Stephen R Carpenter, and Johan Rockström. Social-ecological resilience to coastal disasters. *Science*, 309(5737):1036–1039, 2005.

[44] Jonathan Roughgarden, Robert M May, and Simon A Levin. *Perspectives in ecological theory*. Princeton University Press, 2014.

[45] Kevin Shear McCann. The diversity–stability debate. *Nature*, 405(6783):228–233, 2000.

[46] Rick Durrett. Coexistence in stochastic spatial models. *The Annals of Applied Probability*, pages 477–496, 2009.

[47] Robert M May. Simple mathematical models with very complicated dynamics. *Nature*, 261(5560):459–467, 1976.

[48] P Yodzis. The stability of real ecosystems. *Nature*, 289(5799):674–676, 1981.

[49] Katharine Z Coyte, Jonas Schluter, and Kevin R Foster. The ecology of the microbiome: networks, competition, and stability. *Science*, 350(6261):663–666, 2015.

[50] Katharine Z Coyte, Hervé Tabuteau, Eamonn A Gaffney, Kevin R Foster, and William M Durham. Microbial competition in porous environments can select against rapid biofilm growth. *Proceedings of the National Academy of Sciences*, page 201525228, 2016.

[51] Richard A Holley and Thomas M Liggett. Ergodic theorems for weakly interacting infinite systems and the voter model. *The annals of probability*, pages 643–663, 1975.

[52] J Theodore Cox. Coalescing random walks and voter model consensus times on the torus in zd. *The Annals of Probability*, pages 1333–1366, 1989.

[53] Vishal Sood and Sidney Redner. Voter model on heterogeneous graphs. *Physical review letters*, 94(17):178701, 2005.

[54] Aleksandr Mikhailovich Lyapunov. The general problem of the stability of motion. *International Journal of Control*, 55(3):531–534, 1992.

[55] Craig G Rieger, David I Gertman, and Miles A McQueen. Resilient control systems: next generation design research. In *2009 2nd Conference on Human System Interactions*, pages 632–636. IEEE, 2009.

[56] H Eugene Stanley. Scaling, universality, and renormalization: Three pillars of modern critical phenomena. *Reviews of modern physics*, 71(2):S358, 1999.

[57] Sergey N Dorogovtsev, Alexander V Goltsev, and José FF Mendes. Critical phenomena in complex networks. *Reviews of Modern Physics*, 80(4):1275, 2008.

[58] Didier Sornette. *Critical phenomena in natural sciences: chaos, fractals, selforganization and disorder: concepts and tools*. Springer Science & Business Media, 2006.

[59] C Wissel. A universal law of the characteristic return time near thresholds. *Oecologia*, 65(1):101–107, 1984.

[60] Egbert H Van Nes and Marten Scheffer. Slow recovery from perturbations as a generic indicator of a nearby catastrophic shift. *The American Naturalist*, 169(6):738–747, 2007.

[61] Uri Alon. *An introduction to systems biology: design principles of biological circuits*. CRC press, 2006.

[62] J Nathaniel Holland, Donald L DeAngelis, and Judith L Bronstein. Population dynamics and mutualism: functional responses of benefits and costs. *The American Naturalist*, 159(3):231–244, 2002.

[63] Romualdo Pastor-Satorras and Alessandro Vespignani. Epidemic spreading in scale-free networks. *Physical review letters*, 86(14):3200, 2001.

[64] Steve Carpenter, Brian Walker, J Marty Anderies, and Nick Abel. From metaphor to measurement: resilience of what to what? *Ecosystems*, 4(8):765–781, 2001.

[65] Michael Rutter. Psychosocial resilience and protective mechanisms. *American journal of orthopsychiatry*, 57(3):316, 1987.

[66] Rudolf P Rohr, Serguei Saavedra, and Jordi Bascompte. On the structural stability of mutualistic systems. *Science*, 345(6195):1253497, 2014.

[67] Jordi Bascompte, Pedro Jordano, Carlos J Melián, and Jens M Olesen. The nested assembly of plant–animal mutualistic networks. *Proceedings of the National Academy of Sciences*, 100(16):9383–9387, 2003.

[68] Virginia Domínguez-García and Miguel A Muñoz. Ranking species in mutualistic networks. *Scientific reports*, 5:8182, 2015.

[69] Ugo Bastolla, Miguel A Fortuna, Alberto Pascual-García, Antonio Ferrera, Bartolo Luque, and Jordi Bascompte. The architecture of mutualistic networks minimizes competition and increases biodiversity. *Nature*, 458(7241):1018–1020, 2009.

[70] Paulo R Guimarães Jr, Mathias M Pires, Pedro Jordano, Jordi Bascompte, and John N Thompson. Indirect effects drive coevolution in mutualistic networks. *Nature*, 2017.

[71] Cang Hui. Carrying capacity, population equilibrium, and environment's maximal load. *Ecological Modelling*, 192(1):317–320, 2006.

[72] Warder Clyde Allee, Orlando Park, Alfred Edwards Emerson, Thomas Park, Karl P Schmidt, et al. *Principles of animal ecology.* Number Edn 1. WB Saundere Co. Ltd., 1949.

[73] Jeff Ollerton, Duncan McCollin, Daphne G Fautin, and Gerald R Allen. Finding nemo: nestedness engendered by mutualistic organization in anemonefish and their hosts. *Proceedings of the Royal Society of London B: Biological Sciences*, 274(1609):591–598, 2007.

[74] Nico Blüthgen, Nigel E Stork, and Konrad Fiedler. Bottom-up control and co-occurrence in complex communities: honeydew and nectar determine a rainforest ant mosaic. *Oikos*, 106(2):344–358, 2004.

[75] Mary T Kalin Arroyo, Juan J Armesto, and Richard B Primack. Community studies in pollination ecology in the high temperate andes of central chile ii. effect of temperature on visitation rates and pollination possibilities. *Plant systematics and evolution*, 149(3-4):187–203, 1985.

[76] Gilberto M de Mendonça Santos, Cândida M Lima Aguiar, and Marco AR Mello. Flower-visiting guild associated with the caatinga flora: trophic interaction networks formed by social bees and social wasps with plants. *Apidologie*, 41(4):466–475, 2010.

[77] Jordi Bascompte. Web of life. *http://www.web-of-life.es/*.

[78] Karoline Faust and Jeroen Raes. Microbial interactions: from networks to models. *Nature reviews. Microbiology*, 10(8):538, 2012.

[79] Vito Volterra. Leçons sur la théorie mathématique de la lutte pour la vie. *Bull. Amer. Math. Soc. 42 (1936), 304-305 DOI: http://dx. doi. org/10.1090/S0002-9904-1936-06292-0 PII*, pages 0002–9904, 1936.

[80] Samir Suweis, Jacopo Grilli, and Amos Maritan. Disentangling the effect of hybrid interactions and of the constant effort hypothesis on ecological community stability. *Oikos*, 123(5):525–532, 2014.

[81] Si Tang and Stefano Allesina. Reactivity and stability of large ecosystems. *Frontiers in Ecology and Evolution*, 2:21, 2014.

[82] Stephen P Hubbell et al. unified neutral theory of biodiversity and biogeography. 2001.

[83] Javier García-Algarra, Javier Galeano, Juan Manuel Pastor, José María Iriondo, and José J Ramasco. Rethinking the logistic approach for population dynamics of mutualistic interactions. *Journal of theoretical biology*, 363:332–343, 2014.

[84] Sandro Azaele, Samir Suweis, Jacopo Grilli, Igor Volkov, Jayanth R Banavar, and Amos Maritan. Statistical mechanics of ecological systems: Neutral theory and beyond. *Reviews of Modern Physics*, 88(3):035003, 2016.

[85] G Evelyn Hutchinson. The paradox of the plankton. *The American Naturalist*, 95(882):137–145, 1961.

[86] Peter Chesson. Mechanisms of maintenance of species diversity. *Annual review of Ecology and Systematics*, 31(1):343–366, 2000.

[87] Andrea Giometto, Marco Formentin, Andrea Rinaldo, Joel E Cohen, and Amos Maritan. Sample and population exponents of generalized taylor's law. *Proceedings of the National Academy of Sciences*, 112(25):7755–7760, 2015.

[88] Pincelli M Hull, Simon AF Darroch, and Douglas H Erwin. Rarity in mass extinctions and the future of ecosystems. *Nature*, 528(7582):345, 2015.

[89] Gerardo Ceballos, Paul R Ehrlich, Anthony D Barnosky, Andrés García, Robert M Pringle, and Todd M Palmer. Accelerated modern human–induced species losses: Entering the sixth mass extinction. *Science advances*, 1(5):e1400253, 2015.

[90] Lotka Alfred. Elements of physical biology. 1925.

[91] Vito Volterra. Fluctuations in the abundance of a species considered mathematically. *Nature*, 118(2972):558–560, 1926.

[92] BS Goh and LS Jennings. Feasibility and stability in randomly assembled lotka-volterra models. *Ecological Modelling*, 3(1):63–71, 1977.

[93] György Barabás, Simone Pigolotti, Mats Gyllenberg, Ulf Dieckmann, and Géza Meszéna. Continuous coexistence or discrete species? a new review of an old question. 2012.

[94] Alan J McKane and Timothy J Newman. Stochastic models in population biology and their deterministic analogs. *Physical Review E*, 70(4):041902, 2004.

[95] John H Vandermeer. Niche theory. *Annual Review of Ecology and Systematics*, 3(1):107–132, 1972.

[96] Matthew A Leibold. The niche concept revisited: mechanistic models and community context. *Ecology*, 76(5):1371–1382, 1995.

[97] Michael Phillip Austin. Continuum concept, ordination methods, and niche theory. *Annual review of ecology and systematics*, 16(1):39–61, 1985.

[98] Robert Harding Whittaker and Simon A Levin. *Niche: theory and application*, volume 3. Halsted Pr, 1975.

[99] Shiri Freilich, Raphy Zarecki, Omer Eilam, Ella Shtifman Segal, Christopher S Henry, Martin Kupiec, Uri Gophna, Roded Sharan, and Eytan Ruppin. Competitive and cooperative metabolic interactions in bacterial communities. *Nature communications*, 2:589, 2011.

[100] Michel Loreau, Shahid Naeem, Pablo Inchausti, J Bengtsson, JP Grime, A Hector, DU Hooper, MA Huston, D Raffaelli, B Schmid, et al. Biodiversity and ecosystem functioning: current knowledge and future challenges. *science*, 294(5543):804–808, 2001.

[101] Helmut Hillebrand and Birte Matthiessen. Biodiversity in a complex world: consolidation and progress in functional biodiversity research. *Ecology letters*, 12(12):1405–1419, 2009.

[102] Crawford S Holling. Some characteristics of simple types of predation and parasitism1. *The Canadian Entomologist*, 91(7):385–398, 1959.

[103] Jacopo Grilli, György Barabás, Matthew J Michalska-Smith, and Stefano Allesina. Higher-order interactions stabilize dynamics in competitive network models. *Nature*, 548(7666):210, 2017.

[104] Jacopo Grilli, Tim Rogers, and Stefano Allesina. Modularity and stability in ecological communities. *Nature communications*, 7, 2016.

[105] Stefano Allesina, Jacopo Grilli, György Barabás, Si Tang, Johnatan Aljadeff, and Amos Maritan. Predicting the stability of large structured food webs. *Nature communications*, 6, 2015.

[106] Robert M May. Will a large complex system be stable? *Nature*, 238(5364):413–414, 1972.

[107] M Vallade and B Houchmandzadeh. Analytical solution of a neutral model of biodiversity. *Physical Review E*, 68(6):061902, 2003.

[108] Igor Volkov, Jayanth R Banavar, Stephen P Hubbell, and Amos Maritan. Neutral theory and relative species abundance in ecology. *Nature*, 424:1035–1037, 2003.

[109] David Alonso, Rampal S Etienne, and Alan J McKane. The merits of neutral theory. *Trends in ecology & evolution*, 21(8):451–457, 2006.

[110] Simone Pigolotti and Massimo Cencini. Speciation-rate dependence in species–area relationships. *Journal of theoretical biology*, 260(1):83–89, 2009.

[111] Enrico Bertuzzo, Samir Suweis, Lorenzo Mari, Amos Maritan, Ignacio Rodríguez-Iturbe, and Andrea Rinaldo. Spatial effects on species persistence and implications for biodiversity. *Proceedings of the National Academy of Sciences*, 108(11):4346–4351, 2011.

[112] Bahram Houchmandzadeh. Neutral aggregation in finite-length genotype space. *Physical Review E*, 95(1):012402, 2017.

[113] Nicolaas Godfried Van Kampen. *Stochastic processes in physics and chemistry*, volume 1. Elsevier, 1992.

[114] Crispin W Gardiner. *Stochastic methods*. Springer-Verlag, Berlin–Heidelberg–New York–Tokyo, 1985.

[115] Alan McKane, David Alonso, and Ricard V Solé. Mean-field stochastic theory for species-rich assembled communities. *Physical Review E*, 62(6):8466, 2000.

[116] Richard Durrett and Simon A Levin. Stochastic spatial models: a user's guide to ecological applications. *Philosophical Transactions of the Royal Society of London B: Biological Sciences*, 343(1305):329–350, 1994.

[117] Rick Durrett. Stochastic spatial models. *SIAM review*, 41(4):677–718, 1999.

[118] Claudio Castellano, Santo Fortunato, and Vittorio Loreto. Statistical physics of social dynamics. *Reviews of modern physics*, 81(2):591, 2009.

[119] Oscar A Pinto and Miguel A Munoz. Quasi-neutral theory of epidemic outbreaks. *PloS one*, 6(7):e21946, 2011.

[120] Anna Posfai, Thibaud Taillefumier, and Ned S Wingreen. Metabolic trade-offs promote diversity in a model ecosystem. *Physical Review Letters*, 118(2):028103, 2017.

[121] Stewart N Ethier and Thomas G Kurtz. *Markov processes: characterization and convergence*, volume 282. John Wiley & Sons, 2009.

[122] Eugene Seneta. *Non-negative matrices and Markov chains*. Springer Science & Business Media, 2006.

[123] Jordi Bascompte and Pedro Jordano. Plant-animal mutualistic networks: the architecture of biodiversity. *Annu. Rev. Ecol. Evol. Syst.*, 38:567–593, 2007.

[124] Claudio Borile, Paolo Dai Pra, Markus Fischer, Marco Formentin, and Amos Maritan. Time to absorption for a heterogeneous neutral competition model. *Journal of Statistical Physics*, 156(1):119–130, 2014.

[125] Carl D Meyer. *Matrix analysis and applied linear algebra*, volume 2. Siam, 2000.

[126] Gipsi Lima-Mendez, Karoline Faust, Nicolas Henry, Johan Decelle, Sébastien Colin, Fabrizio Carcillo, Samuel Chaffron, J Cesar Ignacio-Espinosa, Simon Roux, Flora Vincent, et al. Determinants of community structure in the global plankton interactome. *Science*, 348(6237):1262073, 2015.

[127] Richard R Stein, Debora S Marks, and Chris Sander. Inferring pairwise interactions from biological data using maximum-entropy probability models. *PLoS Comput Biol*, 11(7):e1004182, 2015.

[128] Soheil Feizi, Daniel Marbach, Muriel Médard, and Manolis Kellis. Network deconvolution as a general method to distinguish direct dependencies in networks. *Nature biotechnology*, 31(8):726, 2013.

[129] Mathew A Leibold, Marcel Holyoak, Nicolas Mouquet, Priyanga Amarasekare, Jonathan M Chase, Martha F Hoopes, Robert D Holt, Jonathan B Shurin, Richard Law, David Tilman, et al. The metacommunity concept: a framework for multi-scale community ecology. *Ecology letters*, 7(7):601–613, 2004.

[130] Rachata Muneepeerakul, Enrico Bertuzzo, Heather J Lynch, William F Fagan, Andrea Rinaldo, and Ignacio Rodriguez-Iturbe. Neutral metacommunity models predict fish diversity patterns in mississippi-missouri basin. *Nature*, 453(7192):220, 2008.

[131] Albert-Laszlo Barabasi and Zoltan N Oltvai. Network biology: understanding the cell's functional organization. *Nature reviews genetics*, 5(2), 2004.

[132] Hiroaki Kitano. Systems biology: a brief overview. *Science*, 295(5560):1662–1664, 2002.

[133] Markus J Herrgård, Neil Swainston, Paul Dobson, Warwick B Dunn, K Yalcin Arga, Mikko Arvas, Nils Blüthgen, Simon Borger, Roeland Costenoble, Matthias Heinemann, et al. A consensus yeast metabolic network reconstruction obtained from a community approach to systems biology. *Nature biotechnology*, 26(10):1155, 2008.

[134] Igor Volkov, Jayanth R Banavar, Stephen P Hubbell, and Amos Maritan. Inferring species interactions in tropical forests. *Proceedings of the National Academy of Sciences*, 106(33):13854–13859, 2009.

[135] David Lazer, Alex Sandy Pentland, Lada Adamic, Sinan Aral, Albert Laszlo Barabasi, Devon Brewer, Nicholas Christakis, Noshir Contractor, James Fowler, Myron Gutmann, et al. Life in the network: the coming age of computational social science. *Science (New York, NY)*, 323(5915):721, 2009.

[136] David Liben-Nowell and Jon Kleinberg. The link-prediction problem for social networks. *journal of the Association for Information Science and Technology*, 58(7):1019–1031, 2007.

[137] Nathan Eagle, Alex Sandy Pentland, and David Lazer. Inferring friendship network structure by using mobile phone data. *Proceedings of the national academy of sciences*, 106(36):15274–15278, 2009.

[138] Roderick C Dewar, Charles H Lineweaver, Robert K Niven, and Klaus Regenauer-Lieb. *Beyond the Second Law: Entropy Production and Non-equilibrium Systems*. Springer, 2013.

[139] Edwin T Jaynes. *Probability theory: The logic of science*. Cambridge university press, 2003.

[140] Timothy R Lezon, Jayanth R Banavar, Marek Cieplak, Amos Maritan, and Nina V Fedoroff. Using the principle of entropy maximization to infer genetic interaction networks from gene expression patterns. *Proceedings of the National Academy of Sciences*, 103(50):19033–19038, 2006.

[141] Jonathan Friedman and Eric J Alm. Inferring correlation networks from genomic survey data. *PLoS Comput Biol*, 8(9):e1002687, 2012.

[142] Thilo Penzl. Numerical solution of generalized lyapunov equations. *Advances in Computational Mathematics*, 8(1):33–48, 1998.